別紙４
研究成果の刊行に関する一覧表

雑誌

発表者氏名	論文タイトル名	発表誌名	巻号	ページ	出版年
Azusa Yano, Shingo Oda, Tatsuki Fukami, Miki Nakajima, and Tsuyoshi Yokoi	Development of a cell-based assay system considering drug metabolism and immune- and inflammatory-related factors for the risk assessment of drug-induced liver injury.	***Txicology Letters***		in press	2014
Shohei Takai, Satonori Higuchi, Azusa Yano, Koichi Tsuneyama, Tatsuki Fukami, Miki Nakajima, and Tsuyoshi Yokoi	Involvement of immune- and inflammatory-related factors in flucloxacillin-induced liver injury in mice.	***Journal of Applied Toxicology***		in press	2014
Shinya Endo, Azusa Yano, Tatsuki Fukami, Miki Nakajima, and Tsuyoshi Yokoi	Involvement of miRNAs in the early phase of halothane-induced liver injury.	***Toxicology***	319	75-84	2014
Shingo Oda, Tatsuki Fukami, Tsuhyoshi Yokoi, and Miki Nakajima	Epigenetic regulation of the tissue-specific expression of human UDP-glucuronosyltransferase (UGT) 1A10.	***Biochemical Pharmacology***	87	660-667	2014
Kentaro Matsuo, Eita Sasaki, Satonori Higuchi, Shohei Takai, Koichi Tsuneyama, Tatsuki Fukami, Miki Nakajima and Tsuyoshi Yokoi	Involvement of oxidative stress and immune- and inframmation-related factors in azathioprine-induced liver injury.	***Txicology Letters***	224	215-224	2014
Taishi Miyashita, Kento Kimura, Tatsuki Fukami, Miki Nakajima and Tsuyoshi Yokoi	Evaluation and mechanistic analysis of the cytotoxicity of the acyl glucuronide of nonsteroidal anti-inflammatory drugs.	***Drug Metabolism and Disposition***	42	1-8	2014
Eita Sasaki, Kentaro Matsuo, Azumi Iida, Koichi Tsuneyama, Tatsuki Fukami, Miki Nakajima, and Tsuyoshi Yokoi	A novel mouse model for phenytoin-induced liver injury: involvement of immune-related factors and P450-mediated metabolism.	***Toxicological Sciences***	136	250-263	2013

Kei Takahashi, Shin-ichi Yokota, Naoyuki Tatsumi, Tatsuki Fukami, Tsuyoshi Yokoi, and Miki Nakajima	Cigarette smoking substantially alters plasma microRNA profiles in healthy subjects.	***Toxicology and Applied Pharmacology***	272	154-160	2013
Ryota Higuchi, Tatsuki Fukami, Miki Nakajima, and Tsuyoshi Yokoi	Prilocaine- and lidocaine-induced methemoglobinemia is caused by human carbosylesterase-, CYP2E1- and CYP3A4-medicated metabolic activation.	***Drug Metabolism and Disposition***	41	1220-1230	2013
Shingo Oda, Tatsuki Fukami, Tsuyoshi Yokoi, and Miki Nakajima	Epigenetic regulation is a crucial factor in the repression of UGT1A1 expression in human kidney	***Drug Metabolism and Disposition***	41	1738-1743	2013

総説

発表者氏名	論文タイトル名	発表誌名	巻号	ページ	出版年
Tsuyoshi Yokoi and Miki Nakajima	microRNAs as mediators of drug toxicity	Annu. Rev. Pharmacol. Toxicol	53	377-400	2013

VI. 研究成果の刊行物・別刷

1521-009X/41/9/1738–1743$25.00
DRUG METABOLISM AND DISPOSITION

http://dx.doi.org/10.1124/dmd.113.051201
Drug Metab Dispos 41:1738–1743, October 2013

Special Section on Epigenetic Regulation of Drug Metabolizing Enzymes and Transporters

Epigenetic Regulation Is a Crucial Factor in the Repression of UGT1A1 Expression in the Human Kidney

Shingo Oda, Tatsuki Fukami, Tsuyoshi Yokoi, and Miki Nakajima

Drug Metabolism and Toxicology, Faculty of Pharmaceutical Sciences, Kanazawa University, Kakuma-machi, Kanazawa, Japan

Received January 24, 2013; accepted February 11, 2013

ABSTRACT

Human uridine 5′-diphospho-glucuronosyltransferase (UGT) 1A1 catalyzes the metabolism of numerous clinically and pharmacologically important compounds, such as bilirubin and SN-38. UGT1A1 is predominantly expressed in the liver and intestine but not in the kidney. The purpose of this study was to uncover the mechanism of the tissue-specific expression of UGT1A1, focusing on its epigenetic regulation. Bisulfite sequence analysis revealed that the CpG-rich region near the *UGT1A1* promoter (−85 to +40) was hypermethylated (83%) in the kidney, whereas it was hypomethylated (37%) in the liver. A chromatin immunoprecipitation assay demonstrated that histone H3 near the promoter was hypoacetylated in the kidney but hyperacetylated in the liver; this hyperacetylation was accompanied by the recruitment of hepatocyte nuclear factor (HNF) 1α to the promoter. The *UGT1A1* promoter in human kidney-derived HK-2 cells that do not express UGT1A1 was fully methylated, but this promoter was relatively unmethylated in human liver-derived HuH-7 cells that express UGT1A1. Treatment with 5-aza-2′-deoxycytidine (5-aza-dC), an inhibitor of DNA methylation, resulted in an increase of UGT1A1 mRNA expression in both cell types, but the increase was much larger in HK-2 cells than in HuH-7 cells. The transfection of an HNF1α expression plasmid into the HK-2 cells resulted in an increase of UGT1A1 mRNA only in the presence of 5-aza-dC. In summary, we found that DNA hypermethylation, along with histone hypoacetylation, interferes with the binding of HNF1α, resulting in the defective expression of UGT1A1 in the human kidney. Thus, epigenetic regulation is a crucial determinant of tissue-specific expression of UGT1A1.

Introduction

Uridine 5′-diphospho-glucuronosyltransferases (UGTs) catalyze the glucuronidation of a large number of endogenous and exogenous compounds. In humans, there are 19 functional UGT enzymes; these enzymes are classified into three subfamilies, UGT1A, UGT2A, and UGT2B (Mackenzie et al., 2005). The *UGT1A* genes, located on chromosome 2q37, contain multiple unique first exons and common exons 2 to 5, and they encode nine kinds of functional UGT1A enzymes (Ritter et al., 1992). The *UGT2* genes, located on chromosome 4q13, comprise six exons that are not shared between the UGT2 family members, with the exception of UGT2A1 and UGT2A2, which are formed by exon sharing as in UGT1A. The *UGT2* genes encode three UGT2A and seven UGT2B functional enzymes.

Human UGTs show tissue-specific expression. Although most UGTs are predominantly expressed in the liver, UGT1A7, UGT1A8, and UGT1A10 are exclusively expressed in the gastrointestinal tract (Strassburg et al., 1997, 1998). UGT1A1 is expressed in the liver, small intestine, and colon, but not in the kidney (Nakamura et al., 2008; Ohno and Nakajin, 2009; Court et al., 2012). The expression of UGT2A1 and 2A2 are limited to the olfactory epithelium (Court et al., 2012). UGT2B7 is abundantly expressed in the liver, kidney, small intestine, and colon, whereas UGT2B10 is expressed only in the liver (Court et al., 2012). To understand the underlying mechanisms of the tissue specific-expression of UGTs, some studies were conducted with a focus on transcriptional regulation (Gardner-Stephen and Mackenzie, 2008; Mackenzie et al., 2010). It has been demonstrated that the intestine-specific transcription factor, caudal-type homeobox protein 2 (Cdx2), as well as Sp1 and hepatocyte nuclear factor (HNF) 1α regulate UGT1A8 and 1A10 expression in the intestine (Gregory et al., 2004). HNF1α and Cdx2 cooperatively regulate UGT2B7 expression in the intestine, whereas HNF1α and octamer transcription factor-1 cooperatively regulate its expression in the liver and kidney (Gregory et al., 2006). HNF1α is also involved in the regulation of UGT1A1 expression in the liver (Bernard et al., 1999). Thus, knowledge of the transcriptional regulation of the tissue-specific expression of the UGTs is accumulating.

However, a question that has yet to be answered is why UGT1A1 is not expressed in the kidney, even though HNF1α is expressed in this tissue (Rey-Campos et al., 1991). In this study, we sought

dx.doi.org/10.1124/dmd.113.051201.

ABBREVIATIONS: 5-aza-dC, 5-aza-2′-deoxycytidine; ChIP, chromatin immunoprecipitation; GAPDH, glyceraldehyde-3-phosphate dehydrogenase; HNF, hepatocyte nuclear factor; PCR, polymerase chain reaction; TSA, trichostatin A; UGT, uridine 5′-diphospho-glucuronosyltransferase.

to clarify the mechanisms underlying the defective expression of UGT1A1, with a focus on epigenetic regulation. It is known that epigenetic changes, including DNA methylation and histone modification, are key regulators of tissue-dependent gene expression (Shiota, 2004; Ohgane et al., 2008). Supporting our hypothesis, a previous study found that the DNA methylation status of the proximal promoter region of the *UGT1A1* gene affects UGT1A1 expression in colon cancer cell lines (Gagnon et al., 2006). We investigated whether DNA methylation of the promoter and histone modification might be determinants of the tissue-specific expression of human UGT1A1.

Materials and Methods

Materials. 5-Aza-2'-deoxycytidine (5-Aza-dC) and trichostatin A (TSA) were purchased from Sigma-Aldrich (St. Louis, MO). Goat anti-human HNF1α polyclonal antibody (C-19), mouse anti-β-actin monoclonal antibody (C-14), and control rabbit and goat IgGs were purchased from Santa Cruz Biotechnology (Santa Cruz, CA). Rabbit anti-human acetyl histone H3 polyclonal antibody was purchased from Millipore (Billerica, MA). Primers were commercially synthesized at Hokkaido System Science (Sapporo, Japan). All other chemicals and solvents were of the highest grade commercially available.

Human Tissues. Human liver and kidney samples from five Japanese donors (donor 1, an 80-year-old woman; donor 2, a 54-year-old man; donor 3, a 39-year-old woman; donor 4, a 13-year-old boy; donor 5, a 40-year-old man) were obtained from autopsy materials that were discarded after pathologic investigation. The use of the human livers and kidneys was approved by the ethics committees of Kanazawa University (Kanazawa, Japan) and Iwate Medical University (Morioka, Japan).

Cell Culture. Human kidney tubular epithelial cell line HK-2 and human hepatocellular carcinoma cell line HuH-7 were obtained from the American Type Culture Collection (Manassas, VA) and the RIKEN BioResource Center (Ibaraki, Japan), respectively. These cells were cultured as previously described (Nakamura et al., 2008).

RNA Isolation and Real-Time Polymerase Chain Reaction. Total RNA was isolated from human liver and kidney samples using RNAiso (Takara Bio, Otsu, Japan) according to the manufacturer's protocol. The cDNA was synthesized from the total RNA using ReverTra Ace (Toyobo, Osaka, Japan). The UGT1A1 mRNA levels were determined by real-time polymerase chain reaction (PCR) and normalized with glyceraldehyde-3-phosphate dehydrogenase (GAPDH) mRNA levels as described previously (Izukawa et al., 2009).

Genomic DNA Extraction and Bisulfite Reaction. Genomic DNA samples were prepared from human liver (donor 3) and kidney (donor 1) samples, cell lines, or human hepatocytes (HH268, a 54-year-old Caucasian woman; Tissue Transformation Technologies, Edison, NJ) with a Gentra Puregene Tissue kit (Qiagen, Valencia, CA). Five hundred nanograms of genomic DNA digested with *EcoR* I were treated with bisulfite using the EZ DNA Methylation kit (Zymo Research, Orange, CA). The DNA fragment near the transcription start site of the *UGT1A1* gene was amplified by PCR using the primer pair shown in Table 1. The PCR products were cloned into the pT7Blue T-Vector (Novagen, Madison, WI), and randomly picked clones were sequenced. The DNA methylation status of the sequence was analyzed using the web-based tool QUMA (Kumaki et al., 2008).

Chromatin Immunoprecipitation Assay. The chromatin immunoprecipitation (ChIP) assay was performed using the ChIP assay kit (Millipore) with slight modifications. Approximately 200 mg of frozen human liver (donor 3) or kidney (donor 1) was minced on ice and suspended in 1% (v/v) formaldehyde to cross-link proteins to DNA. After centrifugation, the precipitate was resuspended in cell lysis buffer and homogenized using a Dounce homogenizer. After centrifugation, the precipitate was resuspended in nuclei lysis buffer and sonicated to shear the genomic DNA. After centrifugation, the supernatant (100 μl) was diluted 10-fold with immunoprecipitation dilution buffer and incubated with Dynabeads protein G (Life Technologies, Gaithersburg, MD) conjugated to antibodies against acetylated histone H3 (5 μg) or HNF1α (2 μg). A proportion of the diluted supernatant was kept as an input. The Dynabeads protein G was precipitated and washed sequentially one time each with a low-salt immune complex wash buffer, a high-salt immune complex buffer, and a lithium chloride immune complex buffer. The DNA-protein complex was eluted with elution buffer twice, and the cross-links were reversed by adding sodium chloride. DNA was extracted by phenol-chloroform extraction and ethanol precipitation. The -118 to $+91$ region of the *UGT1A1* gene was amplified by real-time PCR with the primers shown in Table 1. The protocol for the PCR was as follows: 95°C for 30 seconds, followed by 45 cycles of 94°C for 4 seconds and 62°C for 20 seconds. DNA extraction and real-time PCR were also performed for the input samples, and the data were used as a control to evaluate the enrichment of DNA in the immunoprecipitates.

Construction of an HNF1α Expression Plasmid. Human HNF1α cDNA was amplified by PCR using the primer pair shown in Table 1 and human liver cDNA as a template. The PCR product was subcloned into the pTARGET vector (Promega, Madison, MI). The nucleotide sequence was confirmed by DNA sequencing analysis.

Chemical Treatment and Transfection of Expression Plasmid into the Cells. HK-2 and HuH-7 cells were seeded onto a 12-well plate at 0.5×10^5 cells/well and incubated for 24 hours. For dose response experiments, the cells were treated with 0.01, 0.1, 1, or 10 μM 5-aza-dC for 120 hours or treated with 50, 100, or 300 nM TSA for 24 hours and then subjected to RNA isolation. For the overexpression of HNF1α, the cells were transiently transfected with 0.5 μg of an HNF1α expression plasmid or an empty pTARGET plasmid using the X-tremeGENE HP DNA transfection reagent (Roche Applied Science, Indianapolis, IN). After 12 hours, the cells were treated with 0.1 μM 5-aza-dC for 96 hours, followed by treatment with TSA for an additional 24 hours. The UGT1A1 mRNA levels were determined as previously described.

Preparation of Nuclear Extract and Immunoblot Analysis of HNF1α. Nuclear extract was prepared from HK-2 and HuH-7 cells transfected with the HNF1α expression plasmid or empty plasmid using NE-PER Nuclear and Cytoplasmic Extraction Reagents (Thermo Fisher Scientific, Rockford, IL) according to the manufacturer's protocols. The protein concentration

TABLE 1

Oligonucleotides used for the UGT1A1 bisulfite analysis and ChIP assay and for the cloning of HNF1α

Nucleotides are numbered with the transcription start site designated as +1 in the *UGT1A1* genomic DNA sequence and base A in the initiation codon ATG designated as +1 in the HNF1α cDNA sequence.

Oligonucleotides	5' to 3' Sequence	Position
Bisulfite analysis of UGT1A1		
Forward	TTTGTGGATTGATAGTTTTTTATAG	−113 to −89
Reverse	CAATAACTACCATCCACTAAAATC	+134 to +111
ChIP assay of UGT1A1		
Forward	CTACCTTTGTGGACTGACAGC	−118 to −98
Reverse	CAACAGTATCTTCCCAGCATG	+111 to +91
Cloning of HNF1α		
Forward	GCAGCCGAGCCATGGTTTCT	−11 to +9
Reverse	GGTGCCGTGGTTACTGGGA	+1906 to +1888

ChIP, chromatin immunoprecipitation; HNF, hepatocyte nuclear factor; UGT, uridine 5'-diphospho-glucuronosyltransferase.

was determined using Bradford protein assay reagent (Bio-Rad Laboratories, Hercules, CA) with γ-globulin as a standard. The nuclear extract (40 μg) was separated by 7.5% SDS-PAGE and transferred to an Immobilon-P transfer membrane (Millipore). The membranes were probed with goat anti-human HNF1α or rabbit anti-human GAPDH antibodies followed by fluorescent dye-conjugated second antibodies. The membranes were then scanned using the Odyssey Infrared Imaging system (LI-COR Biosciences, Lincoln, NE).

Statistical Analyses. For DNA methylation status, the statistical significance was evaluated by the Mann-Whitney *U*-test or Fisher's exact test using the web-based tool QUMA. For mRNA expression, statistical significance was determined using an unpaired, two-tailed Student's *t* test or one-way analysis of variance followed by Dunnett's test. When the *P* value was less than 0.05, the differences were considered to be statistically significant.

Results

UGT1A1 mRNA Expression in Human Liver and Kidney. UGT1A1 mRNA expression in human liver and kidney was determined by real-time PCR. As shown in Fig. 1, UGT1A1 mRNA was detected in the liver but was negligible in the kidney. The results supported previous studies (Nakamura et al., 2008; Ohno and Nakajin, 2009) that reported the repressed expression of UGT1A1 in the human kidney.

DNA Methylation Status of the *UGT1A1* Promoter Region in Human Liver and Kidney. Genomic DNA extracted from the liver and kidney was treated with bisulfite, and the promoter region of UGT1A1 spanning −113 to +111 was amplified by PCR. The PCR product was subcloned into a vector, and 14 clones from each sample were sequenced. The DNA methylation status of the CpG dinucleotides at −85, −54, −12, +12, +36, and +40 of the *UGT1A1* gene is shown in Fig. 2. In the liver, 31 out of 84 CpG sites (37%) were methylated, whereas in the kidney, 70 out of 84 CpGs (83%) were methylated ($P = 0.07$, Mann-Whitney *U* test). Notably, the methylated CpG sites were biased in five clones in the liver. We surmised that these clones might be from hepatic nonparenchymal cells. Hence, we investigated the DNA methylation status of the *UGT1A1* promoter in human hepatocytes and found that the methylated status was only 24% (20 out of 84 CpG sites). In particular, nucleotide positions −85, −54, and −12 were unmethylated in all hepatocyte clones but were hypermethylated in the kidney ($P < 0.001$; $P < 0.01$; and $P < 0.0001$, respectively; Fisher's exact test). Thus, the DNA methylation status of the UGT1A1 promoter region is different in the liver and kidney.

Histone H3 Acetylation Status and Recruitment of HNF1α to the *UGT1A1* Promoter Region. DNA methylation induces chromatin condensation by recruiting chromatin-remodeling factors, such as methyl-CpG-binding protein and histone deacetylase, thus limiting the access of transcription factors (Bird and Wolffe, 1999). We performed ChIP assays to determine the extent of histone H3 acetylation at the *UGT1A1* promoter in the liver and kidney. In addition, the extent of the recruitment of HNF1α to the *UGT1A1* promoter in the liver and kidney was also determined because it has been demonstrated that HNF1α regulates UGT1A1 expression (Bernard et al., 1999). As

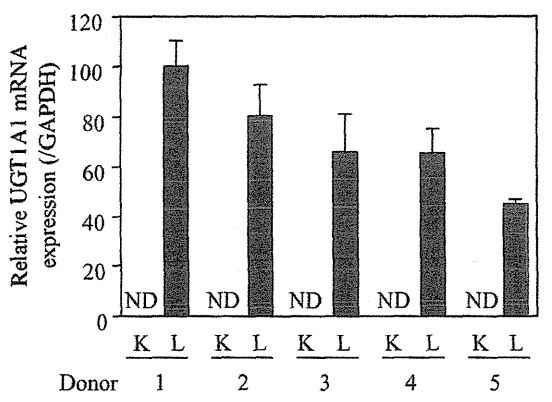

Fig. 1. UGT1A1 mRNA expression in human kidney and liver. The expression levels of UGT1A1 mRNA were determined by real-time PCR and normalized to GAPDH mRNA levels. Each kidney and liver sample with a given number of donors came from the same donors. The values are expressed as relative to the UGT1A1 levels in the liver from donor 1. Each column represents the mean ± S.D. of triplicate determinations. K, kidney; L, liver; ND, not detectable.

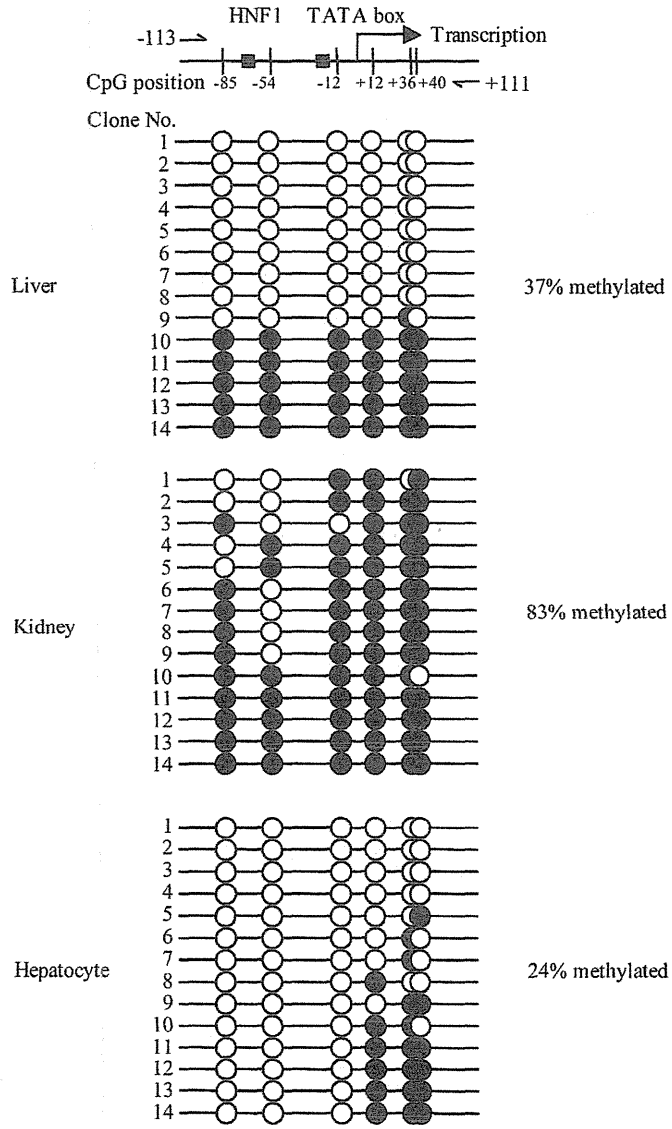

Fig. 2. DNA methylation status of the *UGT1A1* promoter region in human liver, kidney or hepatocytes. Top panel shows a schematic diagram of the *UGT1A1* 5'-flanking region. The vertical lines and numbers represent the position of the cytosine residues of the CpGs relative to the transcription start site as +1. The HNF1 binding site and TATA box are represented by rectangles. Arrows indicate the positions of the primers used for ChIP analysis. Bottom panel shows DNA methylation status of CpG sites. Bisulfite sequencing analysis was performed using genomic DNAs extracted from human liver (donor 3), kidney (donor 1) or hepatocytes (HH268). Fourteen clones from each sample type were sequenced. The open and closed circles represent unmethylated and methylated cytosines, respectively.

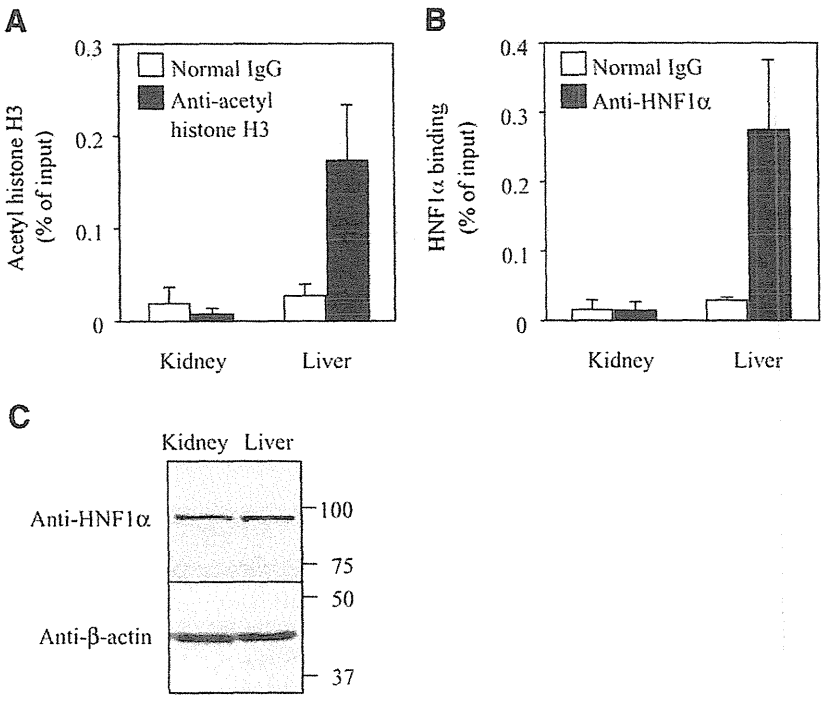

Fig. 3. Histone H3 acetylation and recruitment of HNF1α in the *UGT1A1* promoter region in human kidney and liver. (A and B) ChIP assay of acetyl histone H3 and HNF1α in kidney and liver. Human kidney (donor 1) and liver (donor 3) chromatin was precipitated with anti-acetyl histone H3 antibody (A) or anti-HNF1α antibody (B). The precipitated DNA was quantified by real-time PCR with a primer pair that amplified the region from −118 to +111 of the *UGT1A1* gene. The results are expressed as the percentage of input. Normal rabbit or goat IgGs (open columns) were included as negative controls. (C) Western blot analysis of HNF1α in kidney and liver. Homogenates (50 μg) from kidney and liver samples were subjected to 10% SDS-PAGE and probed with anti-HNF1α or anti-β-actin antibodies. Each column represents the mean ± S.D. of triplicate determinations.

shown in Fig. 3A, acetylated histone H3 was enriched at the *UGT1A1* promoter in the liver but not in the kidney. In addition, it was demonstrated that HNF1α was highly recruited to the *UGT1A1* promoter in the liver but not in the kidney (Fig. 3B). Western blot analysis demonstrated that HNF1α is expressed in kidney and liver equally (Fig. 3C). These results suggest that the DNA hypermethylation in the kidney could be linked to abolished histone H3 acetylation and HNF1α binding.

Effects of the Inhibition of DNA Methylation and Histone Deacetylation and the Transfection of Exogenous HNF1α on UGT1A1 Expression. To investigate the significance of the DNA methylation at the promoter region in the repression of UGT1A1 expression, we performed a series of experiments using cell lines. We selected two cell lines, the human kidney-derived HK-2 line and liver-derived HuH-7 cells. We found that the *UGT1A1* promoter region was hypermethylated (98%) in HK-2 cells but was moderately methylated (47%) in HuH-7 cells ($P < 0.0001$, Fig. 4A). UGT1A1 mRNA was marginally expressed in HK-2 cells but was substantially expressed in HuH-7 cells (~4800-fold difference) (Fig. 4B), suggesting that DNA methylation negatively regulates UGT1A1 expression in HK-2 cells. To investigate whether the inhibition of DNA methylation could induce UGT1A1 expression, the cells were treated with 5-aza-dC, an inhibitor of DNA methylation. Although this treatment increased UGT1A1 mRNA in both cell lines, the induction was higher in HK-2 cells (~400-fold at maximum) than in HuH-7 cells (~6-fold at maximum) (Fig. 4B). We confirmed that 5-aza-dC treatment efficiently decreased the methylation status in HK-2 to 33% ($P < 0.001$) and in HuH-7 cells to 7% ($P < 0.001$) (Fig. 4C).

The UGT1A1 mRNA level in HK-2 cells treated with 0.1 μM 5-aza-dC was still low compared with that in HuH-7 cells. We suspected that HNF1α might be lacking in HK-2 cells, thus causing the lower UGT1A1 levels. Western blot analysis demonstrated that HNF1α is expressed at very low levels in HK-2 cells (Fig. 4D). To investigate the significance of the DNA methylation status in the suppression of UGT1A1 expression, we sought to exogenously express HNF1α in HK-2 cells. The HNF1α protein level was dramatically increased by the transfection of the HNF1α expression plasmid into HK-2 cells (Fig. 4D), but UGT1A1 mRNA expression was not increased (Fig. 4E). These results suggested that DNA methylation inhibits the binding of HNF1α to the promoter of UGT1A1. However, under 5-aza-dC treatment, the overexpression of HNF1α resulted in a significant increase of UGT1A1 mRNA expression (4.3-fold) in HK-2 cells. This phenomenon was not observed in HuH-7 cells, implying that endogenous HNF1α expression levels might be sufficient for UGT1A1 in HuH-7 cells (Fig. 4D).

Finally, we investigated whether histone deacetylation is also involved in the repression of UGT1A1 expression. When the HK-2 and HuH-7 cells were treated with TSA, an inhibitor of histone deacetylation, UGT1A1 mRNA expression was unchanged (Fig. 4E). However, TSA treatment facilitated (by 1.7-fold) the increase of UGT1A1 mRNA by 5-aza-dC treatment in HK-2 cells in the presence of exogenously expressed HNF1α. This result was not observed in HuH-7 cells. Collectively, these results suggest that DNA methylation status, and to a lesser extent histone deacetylation status, are critical determinants of UGT1A1 expression.

Discussion

Human UGT1A1 is predominantly expressed in the liver and the intestine but not in the kidney. Previous studies demonstrated that HNF1α and HNF1β are involved in the constitutive (Bernard et al., 1999) and inducible expression of UGT1A1 (Sugatani et al., 2008) by binding to a site approximately 30 bp upstream of the TATA box. The expression of HNF1α and HNF1β is not confined to the liver, as these genes are expressed in various tissues, including the kidney, intestine, stomach, and pancreas (Harries et al., 2006). Therefore, the reason for the repressed expression of UGT1A1 in the kidney remained to be clarified. To uncover the underlying mechanism, we conducted studies focusing on epigenetic regulation. HNF1α and HNF1β form homodimers or heterodimers and equally *trans*-activate the *UGT1A1* gene (Bernard et al., 1999). Therefore, HNF1α was studied as the representative *UGT1A1* activator.

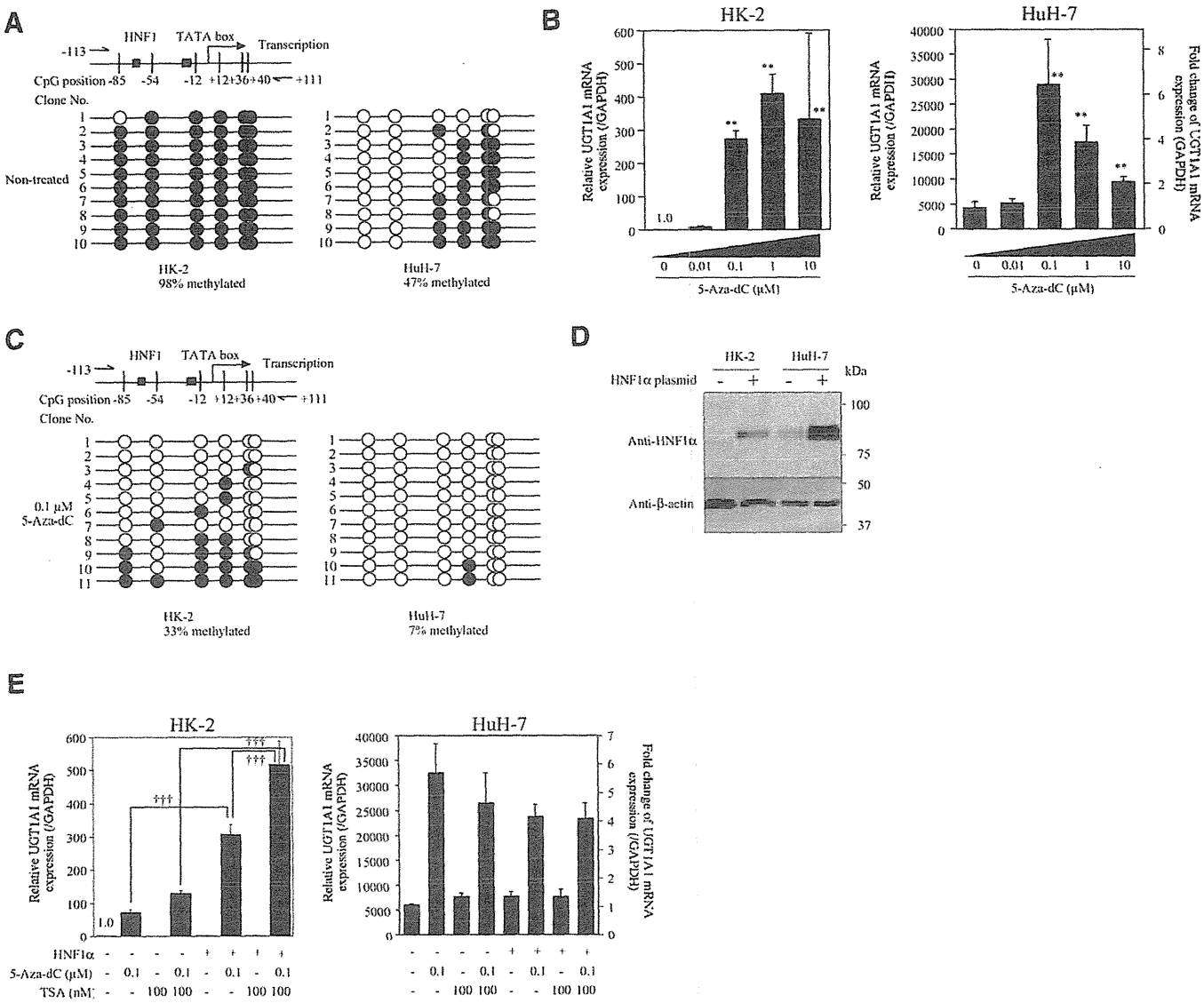

Fig. 4. Effects of 5-aza-dC and/or TSA treatment and transfection of HNF1α on the UGT1A1 expression in HK-2 and HuH-7 cells. (A) DNA methylation status of the *UGT1A1* promoter region in HK-2 and HuH-7 cells. Ten clones each were sequenced. The open and closed circles represent unmethylated and methylated cytosines, respectively. (B) Effects of 5-aza-dC on the UGT1A1 expression in HK-2 and HuH-7 cells. UGT1A1 mRNA level was determined by real-time RT-PCR and normalized with the GAPDH mRNA levels. (C) Effects of 5-aza-dC on the DNA methylation status of the *UGT1A1* promoter region in HK-2 and HuH-7 cells. Bisulfite sequencing analysis was performed using genomic DNA extracted from 5-aza-dC-treated cells. (D) Western blot analysis of HNF1α in HK-2 and HuH-7 cells. Nuclear extracts from HK-2 and HuH-7 cells transfected with HNF1α expression plasmid (+) or empty plasmid (−) were analyzed. (E) Effects of 5-aza-dC and/or TSA treatment and transfection of HNF1α on the UGT1A1 mRNA expression in HK-2 and HuH-7 cells. The cells were transiently transfected with HNF1α expression plasmid (+) or empty plasmid (−), followed by treatment with 5-aza-dC and/or TSA. The expression level of UGT1A1 mRNA was determined by real-time PCR. Data were expressed as relative to UGT1A1 expression compared with nontreated HK-2 cells. Each column represents the mean ± S.D. of triplicate determinations. $^{**}P < 0.01$, compared with nontreated cells; $^{\dagger\dagger\dagger}P < 0.001$.

We found that the CpG island at the promoter region of the *UGT1A1* gene in the kidney was hypermethylated, whereas it was hypomethylated in the liver (Fig. 2). Upon DNA methylation, gene silencing occurs by two mechanisms: 1) the methyl group physically interrupts the binding of transcription factors to their recognition sequences, and 2) methyl-CpG-binding proteins bind to the methylated DNA and recruit co-repressor molecules, including histone deacetylase, to induce chromatin structure condensation (Shiota, 2004). Previously, it was demonstrated by gel shift assay that the methylated CpG sites at the *UGT1A1* promoter did not prevent the binding of HNF1α (Bélanger et al., 2010). In contrast, the present study demonstrated that DNA hypermethylation of the *UGT1A1* promoter in the kidney was accompanied by increased acetylation of histone H3 and defective recruitment of HNF1α (Fig. 3). Therefore, gene silencing of UGT1A1 in the kidney would be due to the latter mechanism with the abolished binding of HNF1α.

Our cell line based study clearly demonstrated the significance of DNA methylation in the regulation of UGT1A1 as follows: 1) substantial expression of UGT1A1 mRNA is observed in HuH-7 cells with DNA hypomethylation status; 2) 5-aza-dC treatment resulted in an increase of UGT1A1 expression that reflected the change in methylation status; and 3) the exogenously expressed HNF1α could increase UGT1A1 expression only in the presence of 5-aza-dC in HK-2 cells. These findings clearly illustrated that unmethylated DNA is a prerequisite for the transcriptional activation of UGT1A1.

The study using TSA demonstrated that histone acetylation is a supplemental factor for transactivation, supporting the general perception (Cameron et al., 1999). In contrast to our study, a previous study reported a significant increase of UGT1A1 mRNA expression following treatment with 3 mM TSA in HepG2 cells (Mackenzie et al., 2010). When we treated the HK-2 and HuH-7 cells with 1 mM TSA, a prominent decrease of cell viability was observed. Thus, it is possible that there are inter-cell line differences in the response toward TSA. Collectively, DNA methylation at the promoter region of UGT1A1 may evoke the condensed chromatin structure through histone deacetylation, thereby inhibiting the binding of such transcription factors as HNF1α. This theory would explain the defective expression of UGT1A1 in kidney, where HNF1α is substantially expressed.

Although the simultaneous overexpression of HNF1α and inhibition of DNA methylation tremendously induced UGT1A1 mRNA in HK-2 cells, the UGT1A1 level was still lower than the level in HuH-7 cells (Fig. 4). It was surmised that some factors regulating UGT1A1 expression might be insufficient in HK-2 cells. Previous studies have reported that pregnane X receptor (Sugatani et al., 2008), glucocorticoid receptor (Usui et al., 2006), constitutive androstane receptor (Sugatani et al., 2008), peroxisome proliferator-activated receptor α (Senekeo-Effenberger et al., 2007), NF-E2-related factor-2 (Yueh and Tukey, 2007), and aryl hydrocarbon receptor (Yueh et al., 2003) are involved in UGT1A1 regulation. It is possible that such factors may be insufficient in HK-2 cells, although experimental proof is required. As another possibility, differences in histone modifications other than acetylation are feasible, namely H3K4 methylation (activating mark), H3K9 methylation (silencing mark), and H3K27 methylation (silencing mark). Thus, such factors might also be involved in the regulation of the basal expression of UGT1A1 in cell lines and tissues.

Each member of UGT1A family has a unique promoter. The tissue-specific expression of UGT1As could be attributed to the differences in their promoter activation (Gong et al., 2001). It is reasonable to assume that UGT isoforms other than UGT1A1 showing tissue-specific expression might also be epigenetically regulated. We are currently working on this issue.

In conclusion, we found that the DNA methylation status of the human *UGT1A1* promoter is different in the liver and kidney. DNA methylation, hypoacetylation of histone H3, and diminished binding of HNF1α could explain the defective expression of UGT1A1 in the kidney. A remaining future challenge is the elucidation of the degree to which UGT1A1 expression is influenced by factors affecting epigenetic status, such as aging, sex, disease, and lifestyle habits.

Acknowledgments

The authors thank Drs. Yasuhiro Aoki and Masataka Takamiya in Iwate Medical University for supplying human tissues.

Authorship Contributions

Participated in research design: Oda, Nakajima, Fukami, Yokoi.

Conducted experiments: Oda.

Performed data analysis: Oda.

Wrote or contributed to the writing of the manuscript: Oda, Nakajima, Yokoi.

References

Bélanger AS, Tojcic J, Harvey M, and Guillemette C (2010) Regulation of *UGT1A1* and *HNF1* transcription factor gene expression by DNA methylation in colon cancer cells. *BMC Mol Biol* **11**:9.

Bernard P, Goudonnet H, Artur Y, Desvergne B, and Wahli W (1999) Activation of the mouse TATA-less and human TATA-containing UDP-glucuronosyltransferase *1A1* promoters by hepatocyte nuclear factor 1. *Mol Pharmacol* **56**:526–536.

Bird AP and Wolffe AP (1999) Methylation-induced repression—belts, braces, and chromatin. *Cell* **99**:451–454.

Cameron EE, Bachman KE, Myöhänen S, Herman JG, and Baylin SB (1999) Synergy of demethylation and histone deacetylase inhibition in the re-expression of genes silenced in cancer. *Nat Genet* **21**:103–107.

Court MH, Zhang X, Ding X, Yee KK, Hesse LM, and Finel M (2012) Quantitative distribution of mRNAs encoding the 19 human UDP-glucuronosyltransferase enzymes in 26 adult and 3 fetal tissues. *Xenobiotica* **42**:266–277.

Gagnon JF, Bernard O, Villeneuve L, Tétu B, and Guillemette C (2006) Irinotecan inactivation is modulated by epigenetic silencing of *UGT1A1* in colon cancer. *Clin Cancer Res* **12**: 1850–1858.

Gardner-Stephen DA and Mackenzie PI (2008) Liver-enriched transcription factors and their role in regulating UDP glucuronosyltransferase gene expression. *Curr Drug Metab* **9**:439–452.

Gong QH, Cho JW, Huang T, Potter C, Gholami N, Basu NK, Kubota S, Carvalho S, Pennington MW, and Owens IS, et al. (2001) Thirteen UDPglucuronosyltransferase genes are encoded at the human UGT1 gene complex locus. *Pharmacogenetics* **11**:357–368.

Gregory PA, Gardner-Stephen DA, Rogers A, Michael MZ, and Mackenzie PI (2006) The caudal-related homeodomain protein Cdx2 and hepatocyte nuclear factor 1α cooperatively regulate the UDP-glucuronosyltransferase 2B7 gene promoter. *Pharmacogenet Genomics* **16**:527–536.

Gregory PA, Lewinsky RH, Gardner-Stephen DA, and Mackenzie PI (2004) Coordinate regulation of the human UDP-glucuronosyltransferase *1A8*, *1A9*, and *1A10* genes by hepatocyte nuclear factor 1α and the caudal-related homeodomain protein 2. *Mol Pharmacol* **65**:953–963.

Harries LW, Ellard S, Stride A, Morgan NG, and Hattersley AT (2006) Isomers of the *TCF1* gene encoding hepatocyte nuclear factor-1 alpha show differential expression in the pancreas and define the relationship between mutation position and clinical phenotype in monogenic diabetes. *Hum Mol Genet* **15**:2216–2224.

Izukawa T, Nakajima M, Fujiwara R, Yamanaka H, Fukami T, Takamiya M, Aoki Y, Ikushiro S, Sakaki T, and Yokoi T (2009) Quantitative analysis of UDP-glucuronosyltransferase (UGT) 1A and UGT2B expression levels in human livers. *Drug Metab Dispos* **37**:1759–1768.

Kumaki Y, Oda M, and Okano M (2008) QUMA: quantification tool for methylation analysis. *Nucleic Acids Res* **36** (Web Server issue):W170-5.

Mackenzie PI, Bock KW, Burchell B, Guillemette C, Ikushiro S, Iyanagi T, Miners JO, Owens IS, and Nebert DW (2005) Nomenclature update for the mammalian UDP glycosyltransferase (*UGT*) gene superfamily. *Pharmacogenet Genomics* **15**:677–685.

Mackenzie PI, Hu DG, and Gardner-Stephen DA (2010) The regulation of UDP-glucuronosyltransferase genes by tissue-specific and ligand-activated transcription factors. *Drug Metab Rev* **42**:99–109.

Nakamura A, Nakajima M, Yamanaka H, Fujiwara R, and Yokoi T (2008) Expression of UGT1A and UGT2B mRNA in human normal tissues and various cell lines. *Drug Metab Dispos* **36**: 1461–1464.

Ohgane J, Yagi S, and Shiota K (2008) Epigenetics: the DNA methylation profile of tissue-dependent and differentially methylated regions in cells. *Placenta* **29** (**Suppl A**):S29-S35.

Ohno S and Nakajin S (2009) Determination of mRNA expression of human UDP-glucuronosyltransferases and application for localization in various human tissues by real-time reverse transcriptase-polymerase chain reaction. *Drug Metab Dispos* **37**:32–40.

Rey-Campos J, Chouard T, Yaniv M, and Cereghini S (1991) vHNF1 is a homeoprotein that activates transcription and forms heterodimers with HNF1. *EMBO J* **10**:1445–1457.

Ritter JK, Yeatman MT, Ferreira P, and Owens IS (1992) Identification of a genetic alteration in the code for bilirubin UDP-glucuronosyltransferase in the *UGT1* gene complex of a Crigler-Najjar type I patient. *J Clin Invest* **90**:150–155.

Senekeo-Effenberger K, Chen S, Brace-Sinnokrak E, Bonzo JA, Yueh MF, Argikar U, Kaeding J, Trottier J, Remmel RP, and Ritter JK, et al. (2007) Expression of the human UGT1 locus in transgenic mice by 4-chloro-6-(2,3-xylidino)-2-pyrimidinylthioacetic acid (WY-14643) and implications on drug metabolism through peroxisome proliferator-activated receptor α activation. *Drug Metab Dispos* **35**:419–427.

Shiota K (2004) DNA methylation profiles of CpG islands for cellular differentiation and development in mammals. *Cytogenet Genome Res* **105**:325–334.

Strassburg CP, Manns MP, and Tukey RH (1998) Expression of the UDP-glucuronosyltransferase 1A locus in human colon. Identification and characterization of the novel extrahepatic UGT1A8. *J Biol Chem* **273**:8719–8726.

Strassburg CP, Oldhafer K, Manns MP, and Tukey RH (1997) Differential expression of the *UGT1A* locus in human liver, biliary, and gastric tissue: identification of *UGT1A7* and *UGT1A10* transcripts in extrahepatic tissue. *Mol Pharmacol* **52**:212–220.

Sugatani J, Mizushima K, Osabe M, Yamakawa K, Kakizaki S, Takagi H, Mori M, Ikari A, and Miwa M (2008) Transcriptional regulation of human *UGT1A1* gene expression through distal and proximal promoter motifs: implication of defects in the *UGT1A1* gene promoter. *Naunyn Schmiedebergs Arch Pharmacol* **377**:597–605.

Usui T, Kuno T, and Mizutani T (2006) Induction of human UDP-glucuronosyltransferase 1A1 by cortisol-GR. *Mol Biol Rep* **33**:91–96.

Yueh MF, Huang YH, Hiller A, Chen S, Nguyen N, and Tukey RH (2003) Involvement of the xenobiotic response element (XRE) in Ah receptor-mediated induction of human UDP-glucuronosyltransferase *1A1*. *J Biol Chem* **278**:15001–15006.

Yueh MF and Tukey RH (2007) Nrf2-Keap1 signaling pathway regulates human UGT1A1 expression *in vitro* and in transgenic *UGT1* mice. *J Biol Chem* **282**:8749–8758.

Address correspondence to: Dr. Miki Nakajima, Drug Metabolism and Toxicology, Faculty of Pharmaceutical Sciences, Kanazawa University, Kakuma-machi, Kanazawa 920-1192, Japan. E-mail: nmiki@p.kanazawa-u.ac.jp

1521-009X/41/6/1220–1230$25.00
DRUG METABOLISM AND DISPOSITION

http://dx.doi.org/10.1124/dmd.113.051714
Drug Metab Dispos 41:1220–1230, June 2013

Prilocaine- and Lidocaine-Induced Methemoglobinemia Is Caused by Human Carboxylesterase-, CYP2E1-, and CYP3A4-Mediated Metabolic Activation[S]

Ryota Higuchi, Tatsuki Fukami, Miki Nakajima, and Tsuyoshi Yokoi

Drug Metabolism and Toxicology, Faculty of Pharmaceutical Sciences, Kanazawa University, Kakuma-machi, Kanazawa, Japan

Received February 22, 2013; accepted March 25, 2013

ABSTRACT

Prilocaine and lidocaine are classified as amide-type local anesthetics for which serious adverse effects include methemoglobinemia. Although the hydrolyzed metabolites of prilocaine (*o*-toluidine) and lidocaine (2,6-xylidine) have been suspected to induce methemoglobinemia, the metabolic enzymes that are involved remain uncharacterized. In the present study, we aimed to identify the human enzymes that are responsible for prilocaine- and lidocaine-induced methemoglobinemia. Our experiments revealed that prilocaine was hydrolyzed by recombinant human carboxylesterase (CES) 1A and CES2, whereas lidocaine was hydrolyzed by only human CES1A. When the parent compounds (prilocaine and lidocaine) were incubated with human liver microsomes (HLM), methemoglobin (Met-Hb) formation was lower than when the hydrolyzed metabolites were incubated with HLM. In addition, Met-Hb formation when prilocaine and *o*-toluidine were incubated with HLM was higher than that when lidocaine and 2,6-xylidine were incubated with HLM. Incubation with diisopropyl fluorophosphate and bis-(4-nitrophenyl) phosphate, which are general inhibitors of CES, significantly decreased Met-Hb formation when prilocaine and lidocaine were incubated with HLM. An anti-CYP3A4 antibody further decreased the residual formation of Met-Hb. Met-Hb formation after the incubation of *o*-toluidine and 2,6-xylidine with HLM was only markedly decreased by incubation with an anti-CYP2E1 antibody. *o*-Toluidine and 2,6-xylidine were further metabolized by CYP2E1 to 4- and 6-hydroxy-*o*-toluidine and 4-hydroxy-2,6-xylidine, respectively, and these metabolites were shown to more efficiently induce Met-Hb formation than the parent compounds. Collectively, we found that the metabolites produced by human CES-, CYP2E1-, and CYP3A4-mediated metabolism were involved in prilocaine- and lidocaine-induced methemoglobinemia.

Introduction

Prilocaine and lidocaine are classified as amide-type local anesthetics, which prevent and relieve pain by interrupting nerve excitation and conduction via direct interaction with voltage-gated Na^+ channels to block the Na^+ current (Lipkind and Fozzard, 2005). In general, prilocaine and lidocaine are safely used in patients, although methemoglobinemia is occasionally induced (Rehman, 2001; Maimo and Redick, 2004). Methemoglobinemia is defined as a methemoglobin (Met-Hb) level >1.0% in the blood. Met-Hb is an abnormal form of hemoglobin in which iron is oxidized from the ferrous (Fe^{2+}) to the ferric state (Fe^{3+}). Because Met-Hb cannot bind and transport oxygen, increased levels of Met-Hb are associated with clinically severe symptoms (Moore et al., 2004). Met-Hb concentrations are normally maintained at roughly 1% of total hemoglobin by the action of Met-Hb reductase (Guay, 2009). Cyanosis usually occurs when Met-Hb concentrations increase above 10% and is followed by anxiety, fatigue, and tachycardia when Met-Hb levels reach 20%–50% of total hemoglobin levels. When Met-Hb levels reach 50%–70% of total hemoglobin levels, coma, and death may occur (Rodriguez et al., 1994).

When prilocaine was used for epidural analgesia and peripheral nerve block, some patients were reported to develop methemoglobinemia (Climie et al., 1967; Vasters et al., 2006). For example, when 288 mg of prilocaine was used in a 19-year-old white woman, her Met-Hb levels were observed to be 37.8% of total hemoglobin levels approximately 4 hours after injection (Kreutz and Kinni, 1983). Fetuses and infants under 6 months of age seem to be more susceptible. Lidocaine also causes methemoglobinemia, although only rarely. In fact, the number of articles that were published from 1949 through 2007 concerning lidocaine-related methemoglobinemia (12 episodes) is lower than the number of articles concerning prilocaine-related methemoglobinemia (68 episodes) (Guay, 2009). In humans, prilocaine and lidocaine are hydrolytically metabolized to the aromatic amines *o*-toluidine and 2,6-xylidine, respectively. These metabolites have been reported to cause increased levels of Met-Hb after intravenous administration to cats or rats (Onji and Tyuma, 1965; Lindstrom et al., 1969). On the basis of the results of these studies, prilocaine and lidocaine hydrolysis pathways have been suggested to play an important role in methemoglobinemia, but the metabolic enzymes that are involved in methemoglobinemia remain to be experimentally characterized. Moreover, it is unclear whether differences in methemoglobinemia frequency after prilocaine and lidocaine treatment are attributable to differences in enzymatic metabolism or differences in the potency of Met-Hb formation by their metabolites.

This work was supported in part by a Grant-in-Aid for Scientific Research from the Japan Society for the Promotion of Science [Grant 23590174].
dx.doi.org/10.1124/dmd.113.051714.
[S]This article has supplemental material available at dmd.aspetjournals.org.

ABBREVIATIONS: AADAC, arylacetamide deacetylase; BNPP, bis-(4-nitrophenyl) phosphate; CES, carboxylesterase; DFP, diisopropyl fluorophosphate; HLM, human liver microsomes; HPLC, high-performance liquid chromatography; Met-Hb, methemoglobin; NADPH-GS, NADPH-generating system; NPR, NADPH-P450 reductase; P450, cytochrome P450.

Esterases, which are expressed in human liver, plasma, and other tissues, contribute to the hydrolysis of approximately 10% of clinically therapeutic drugs, including ester, amide, and thioester bonds (Fukami and Yokoi, 2012). In particular, human carboxylesterases (CES), especially the CES1A and CES2 enzymes, are the major serine esterases that are responsible for the hydrolysis of various drugs and xenobiotics (Imai et al., 2006). Recently, we demonstrated that human arylacetamide deacetylase (AADAC) is involved in the metabolism of drugs such as flutamide, phenacetin, and rifamycins (Watanabe et al., 2009, 2010; Nakajima et al., 2011). We have more recently demonstrated that the hydrolysis of phenacetin by AADAC, which produced *p*-phenetidine, an aromatic amine metabolite, is predominantly involved in the phenacetin-induced formation of Met-Hb (Kobayashi et al., 2012). Thus, it is conceivable that CES1A, CES2, and AADAC are involved in the hydrolysis of prilocaine and lidocaine.

Ganesan et al. (2010) reported that dapsone-hydroxylamine, which is an *N*-hydroxylated metabolite of dapsone, was suspected to be a cause of dapsone-induced methemoglobinemia. The formation of dapsone-hydroxylamine is catalyzed by cytochromes P450 (P450) CYP2C19, CYP2E1, and CYP3A4. We recently reported that metabolic activation by CYP1A2 and CYP2E1 and hydrolysis of AADAC play a predominant role in phenacetin-induced methemoglobinemia (Kobayashi et al., 2012). Thus, it is conceivable that P450(s) are also involved in prilocaine- and lidocaine-induced methemoglobinemia.

On the basis of the aforementioned background studies, in the present study, we investigated the human enzymes responsible for the metabolism of prilocaine and lidocaine to clarify the mechanisms of prilocaine- and lidocaine-induced methemoglobinemia. In addition, the efficiencies of enzymatic metabolism and Met-Hb formation were compared between prilocaine and lidocaine.

Materials and Methods

Chemicals and Reagents. Lidocaine hydrochloride, 2,6-xylidine, *o*-toluidine, 4-hydroxyl-*o*-toluidine, and diisopropyl fluorophosphate (DFP) were purchased from Wako Pure Chemical Industries (Osaka, Japan). 6-Hydroxyl-*o*-toluidine and 4-hydroxyl-2,6-xylidine were purchased from Tokyo Chemical Industry (Tokyo, Japan). Prilocaine hydrochloride and bis-(4-nitrophenyl)-phosphate (BNPP) were obtained from Sigma-Aldrich (St. Louis, MO). Human liver microsomes (HLM; pooled, n = 50); recombinant human CYP1A2, CYP2A6, CYP2C8, CYP2D6 [with NADPH-P450 reductase (NPR)], CYP2B6, CYP2C9, CYP2C19, CYP2E1, and CYP3A4 (with NPR and cytochrome b_5) enzymes expressed in baculovirus-infected insect cells; monoclonal mouse anti-human CYP1A2 antibody; anti-human CYP2E1 antibody; and anti-human CYP3A4 antibody were purchased from BD Gentest (Woburn, MA). Other chemicals were of the highest commercially available grade.

Mouse and Human Red Blood Cells. Animals were maintained in accordance with the National Institutes of Health Guide for Animal Welfare of Japan, and the protocols were approved by the Institutional Animal Care and Use Committee of Kanazawa University, Japan. The use of human red blood cells was approved by the Ethics Committees of Kanazawa University (Kanazawa, Japan). Mouse blood (pooled samples from 5 C57BL/6J mice: 6-week-old male, 20–25 g) that had been obtained from SLC Japan (Hamamatsu, Japan) and human blood samples (from five healthy Japanese volunteers: 22–30-year-old males) were obtained according to our previous report (Kobayashi et al., 2012). All assays were performed immediately after the separation of the red blood cells.

Prilocaine and Lidocaine Hydrolase Activities. Prilocaine and lidocaine hydrolase activities were determined as follows: a typical incubation mixture (final volume of 0.2 ml) contained 100 mM potassium phosphate buffer (pH 7.4) and various enzyme sources (HLM or Sf21 cell homogenates expressing esterases, 0.4 mg/ml). Sf21 cell homogenates expressing CES1A, CES2, or AADAC were prepared as previously described (Fukami et al., 2010; Watanabe et al., 2010). In a preliminary study, we confirmed that the formation rates of *o*-toluidine and 2,6-xylidine from prilocaine and lidocaine, respectively, were linear with respect to protein concentration (< 2.0 mg/ml) and incubation time (<120 minutes). Prilocaine and lidocaine were dissolved in distilled water. The reactions were initiated by the addition of prilocaine and lidocaine (0.2–10 mM for HLM or 0.1–4 mM for Sf21 cell homogenates expressing esterases) after a 2-minute preincubation at 37°C. After a 30-minute incubation, the reactions were terminated by the addition of 10 μl of ice-cold 60% perchloric acid. After removal of the protein by centrifugation at 9500*g* for 5 minutes, a 60-μl portion of the supernatant was subjected to high-performance liquid chromatography (HPLC). The HPLC analysis was performed using an L-7100 pump (Hitachi, Tokyo, Japan), an L-7200 autosampler (Hitachi), an L-7405 UV detector (Hitachi), and a D-2500 Chromato-Integrator (Hitachi) equipped with a Wakopak eco-ODS column (5-μm particle size, 4.6 mm i.d.×150 mm; Wako Pure Chemical Industries). The eluent was monitored at 210 nm with a noise-base clean Uni-3 (Union, Gunma, Japan), which can reduce the noise by integrating the output and increase the signal by 3-fold by differentiating the output and by 5-fold by further amplification with an internal amplifier, resulting in a maximum 15-fold amplification of the signal. The mobile phase was 35% methanol containing 0.2% phosphoric acid and 2.2 mM sodium 1-octanesulfonate. The flow rate was 1.0 ml/min. The column temperature was 35°C. The quantification of *o*-toluidine and 2,6-xylidine was performed by comparing the HPLC peak height with that of an authentic standard. The limit of quantification in the reaction mixture for *o*-toluidine and 2,6-xylidine was 100 nM, with a coefficient of variation <5.6%. The activity at each concentration was determined as the mean value in triplicate. For kinetic analyses of the prilocaine and lidocaine hydrolase activities, the parameters were estimated from the fitted curves with use of a computer program (KaleidaGraph; Synergy Software, Reading, PA) that was designed for use in nonlinear regression analyses.

Met-Hb Formation. A Met-Hb formation assay was conducted according to the methods outlined in our previous study (Kobayashi et al., 2012), with a slight modification. A typical incubation mixture (final volume of 0.2 ml) contained 5% of the mouse red blood cell fraction except in (7), where human red blood cell fraction was used, 100 mM potassium phosphate buffer (pH 7.4), an NADPH-generating system (NADPH-GS: 0.5 mM $NADP^+$, 5 mM glucose 6-phosphate, 5 mM $MgCl_2$, and 1 U/ml glucose-6-phosphate dehydrogenase), and various enzyme sources.

1. To investigate the time-dependence of Met-Hb formation, HLM (1.0 mg/ml) were used as enzyme sources. The reactions were initiated by the addition of prilocaine, lidocaine, *o*-toluidine, or 2,6-xylidine (1 mM) after a 2-minute preincubation at 37°C. After the 0–120-minute incubation at 37°C, the reaction was terminated by placing the samples on ice.
2. To investigate the concentration-dependence of Met-Hb formation, HLM (1.0 mg/ml) were used as enzyme sources. The reactions were initiated by the addition of prilocaine, lidocaine, *o*-toluidine, or 2,6-xylidine (0.01, 0.1, 1, or 10 mM) after a 2-minute preincubation at 37°C. After the 60-minute incubation at 37°C, the reaction was terminated by placing the samples on ice.
3. To determine the P450 enzymes that were involved in prilocaine-, lidocaine-, *o*-toluidine-, and 2,6-xylidine–induced Met-Hb formation, recombinant human P450 enzymes (25 pmol /ml) were used as enzyme sources. The reactions were initiated by the addition of prilocaine (10 mM), lidocaine (10 mM), *o*-toluidine (1 mM), or 2,6-xylidine (1 mM) after a 2-minute preincubation at 37°C. After the 120-minute incubations (prilocaine and lidocaine) and the 60-minute incubations (*o*-toluidine and 2,6-xylidine) at 37°C, the reactions were terminated by placing the samples on ice.
4. To investigate the involvement of various esterase(s) in the HLM, inhibition analyses of prilocaine- and lidocaine-induced Met-Hb formation were performed using the general CES inhibitors DFP and BNPP (Watanabe et al., 2009). HLM (1.0 mg/ml) were used as enzyme sources, and the concentrations of inhibitors were 100 μM. DFP and BNPP were dissolved in distilled water. The reaction conditions were the same as those described in (3).
5. To investigate the involvement of P450 enzymes in the HLM in Met-Hb formation, inhibition analyses of the formation of Met-Hb by prilocaine

(10 mM), lidocaine (10 mM), *o*-toluidine (1 mM), or 2,6-xylidine (1 mM) were performed using anti-P450 antibodies. HLM (0.5 mg/ml) were used as enzyme sources. Ten microliters of antibody-mixtures [4 μl of anti-CYP2E1 antibody mixed with 6 μl of 25 mM Tris-buffer (pH 7.5) or 10 μl of anti-CYP1A2 or anti-CYP3A4 antibody] was incubated on ice for 30 minutes with enzyme sources, after which typical incubation mixtures (final volume of 0.2 ml) that included the antibody mixtures were prepared. To investigate the involvement of P450 enzymes in prilocaine- and lidocaine-induced Met-Hb formation in the absence of a hydrolysis reaction, DFP (100 μM) was added into the incubation mixture. The reaction conditions were the same as those described in (3).

6. To investigate whether the hydroxylated metabolites of *o*-toluidine and 2,6-xylidine induced Met-Hb formation, *o*-toluidine, 4-hydroxy-*o*-toluidine, 6-hydroxy-*o*-toluidine, 2,6-xylidine, and 4-hydroxy-2,6-xylidine (1 mM) were incubated with HLM (1.0 mg/ml) and mouse red blood cells both in the presence and absence of an NADPH-GS. After a 60-minute incubation at 37°C, the reactions were terminated by placing the samples on ice.
7. To investigate the sensitivity of human red blood cells to prilocaine- and lidocaine-induced Met-Hb formation, a Met-Hb formation assay was conducted using human red blood cells instead of mouse red blood cells. HLM (1.0 mg/ml) were used as enzyme sources, and DFP (100 μM) was added into the incubation mixture. The reaction was initiated by the addition of 10 mM prilocaine and lidocaine after a 2-minute preincubation at 37°C. The reaction conditions were the same as those described in (3).

Prilocaine and lidocaine were dissolved in distilled water. *o*-Toluidine and 2,6-xylidine were dissolved in acetonitrile, and the final concentration of acetonitrile in the incubation mixture was 1%. It has been reported that 1% acetonitrile does not inhibit the activities of CYP1A2, CYP2E1, and CYP3A4 (Chauret et al., 1998).

The Met-Hb levels in red blood cells were determined as the percentage of total hemoglobin according to the methods outlined in our previous study (Kobayashi et al., 2012)

Normalizing Met-Hb Formation by P450 Levels in HLM. Met-Hb formation was normalized by the levels of each P450 enzyme in HLM and was calculated using the following equation, where the $P450_{HLM}$ activity and $P450_{expression}$ activity values are the marker activities of each P450 in HLM and recombinant P450 expression systems, respectively:

$$\text{Met-Hb formation normalized by P450 levels in HLM (\%)} = \text{Met-Hb formation by recombinant human P450 expression systems (\%)} \times P450_{HLM} \text{ activity}/P450_{expression}$$

The reaction conditions for Met-Hb formation by recombinant human P450 expression systems were determined as follows: prilocaine, lidocaine (10 mM), and their hydrolyzed metabolites (1 mM) were incubated with each P450 expression system (25 pmol P450/ml), an NADPH-GS, and mouse red blood cells. The incubation time was either 120 minutes (prilocaine and lidocaine) or 60 minutes (*o*-toluidine and 2,6-xylidine).

The reaction conditions for Met-Hb formation in HLM were determined as described in the above paragraph, except HLM (1.0 mg/ml) were used in place of the P450 expression systems. Met-Hb formation was detected as described in (3) above.

Methoxyresorufin *O*-demethylase, chlorzoxazone 6-hydroxylase, and midazolam 1′-hydroxylase activities were measured as markers for the activities of CYP1A2, CYP2E1, and CYP3A4, respectively, by HPLC, according to methods described in our previous reports (Nakajima et al., 2002; Fukami et al., 2007, 2008).

***o*-Toluidine and 2,6-Xylidine Hydroxylase Activities.** The activities of *o*-toluidine and 2,6-xylidine hydroxylase were determined as follows: a typical incubation mixture (final volume of 0.2 ml) contained *o*-toluidine or 2,6-xylidine (4–200 μM), 100 mM potassium phosphate buffer (pH 7.4), an NADPH-GS, and HLM (0.4 mg/ml). In a preliminary study, we confirmed that the formation rates of 4-hydroxyl-*o*-toluidine and 6-hydroxyl-*o*-toluidine from *o*-toluidine, as well as 4-hydroxyl-2,6-xylidine from 2,6-xylidine, in HLM were linear with respect to protein concentration (< 1.0 mg/ml) and incubation time (<60 minutes). *o*-Toluidine and 2,6-xylidine were dissolved in acetonitrile, and the final concentration of acetonitrile in the incubation mixture was 1%.

Inhibition analyses of *o*-toluidine or 2,6-xylidine hydroxylation were performed using anti-P450 antibodies. HLM (0.4 mg/ml) were used as enzyme sources. Eight microliters of antibody-mixtures [3.2 μl of anti-CYP2E1 antibody mixed with 4.8 μl of 25 mM Tris-buffer (pH 7.5) or 8 μl of anti-CYP1A2 or anti-CYP3A4 antibody] was incubated with enzyme sources on ice for 30 minutes. Then, typical incubation mixtures (final volume of 0.2 ml) were prepared by the addition of *o*-toluidine (50 μM) or 2,6-xylidine (30 μM).

The reactions were initiated by the addition of an NADPH-GS after a 2-minute preincubation at 37°C. After a 30-minute incubation, the reactions were terminated by the addition of 10 μl of ice-cold 60% perchloric acid. After removal of the protein by centrifugation at 9500*g* for 5 minutes, a 50-μl portion of the supernatant was subjected to HPLC. The HPLC equipment was the same as that described above. The mobile phase for *o*-toluidine hydroxylation was 8.5% methanol/8% acetonitrile containing 0.2% phosphoric acid and 2.2 mM sodium 1-octanesulfonate, and the mobile phase for 2,6-xylidine hydroxylation was 10% acetonitrile containing 0.11% phosphoric acid and 2.2 mM sodium 1-octanesulfonate. The quantification of the hydroxylated metabolites of *o*-toluidine and 2,6-xylidine was performed by comparing the HPLC peak height with that of an authentic standard. The activity at each concentration was determined as the mean value in triplicate. For kinetic analyses of the *o*-toluidine and 2,6-xylidine hydroxylase activities, the parameters were estimated as described above.

Statistical Methods. Statistical analyses between two and multiple groups were performed using an unpaired, two-tailed Student's *t* test and analysis of variance, followed by Tukey's post-hoc test. $P < 0.05$ was considered to be statistically significant.

Results

Prilocaine and Lidocaine Hydrolase Activities in HLM. Because hydrolysis of prilocaine and lidocaine was suspected to play an important role in methemoglobinemia, we investigated whether microsomes of the human liver, which is the main organ for drug metabolism and expresses various esterases, could hydrolyze prilocaine and lidocaine (Fig. 1, A and B). Data for these hydrolase activities in HLM followed Michaelis-Menten kinetics. The K_m and V_{max} values for the hydrolysis of prilocaine in HLM were 1.15 ± 0.01 mM and 2.46 ± 0.04 nmol/min/mg protein, respectively, resulting in a CL_{int} value of 2.14 ± 0.04 μl/min/mg protein. The K_m and V_{max} values for the hydrolysis of lidocaine in HLM were 0.96 ± 0.06 mM and 0.62 ± 0.01 nmol/min/mg protein, respectively, resulting in a CL_{int} value of 0.66 ± 0.03 μl/min/mg protein (Table 1). Thus, the CL_{int} value for the hydrolysis of prilocaine was shown to be 3.2 higher than that of lidocaine. These results indicated that HLM have a higher metabolic efficiency for prilocaine hydrolysis than for lidocaine hydrolysis.

Prilocaine and Lidocaine Hydrolase Activities by Recombinant Human CES1A and CES2. To confirm that human CES1A, CES2, and AADAC, which are typical serine esterases that are involved in the hydrolysis of numerous drugs, can hydrolyze prilocaine and lidocaine, prilocaine and lidocaine hydrolase activities were measured using recombinant human CES1A, CES2, and AADAC expressed in Sf21 cells (Fig. 1, C and D). Data for these hydrolase activities followed Michaelis-Menten kinetics. The K_m and V_{max} values for prilocaine hydrolase activity by CES1A were 0.31 ± 0.01 mM and 0.40 ± 0.01 nmol/min/mg protein, respectively, resulting in a CL_{int} value of 1.29 ± 0.04 μl/min/mg protein (Table 1). CES2 displayed the prilocaine hydrolase activity with K_m, V_{max}, and CL_{int} values of 0.39 ± 0.01 mM, 0.10 ± 0.00 nmol/min/mg protein, and 0.26 ± 0.00 μl/min/mg protein, respectively. The K_m, V_{max}, and CL_{int} values for lidocaine hydrolysis by CES1A were 0.35 ± 0.06 mM, 0.14 ± 0.00 nmol/min/mg protein, and 0.40 ± 0.02 μl/min/mg

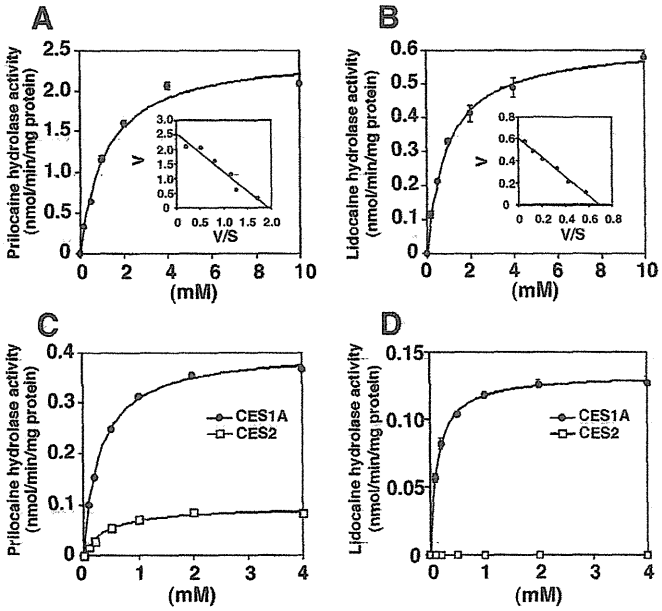

Fig. 1. Kinetic analyses of prilocaine and lidocaine hydrolase activities in HLM and recombinant human CES1A and CES2 expressed in Sf21 cells. HLM (0.4 mg/ml) (A and B) or CES1A and CES2 (0.2 mg/ml) (C and D) were incubated with prilocaine (A and C) and lidocaine (B and D) for 30 minutes. Hydrolase activities for prilocaine and lidocaine were measured by quantitative analyses of *o*-toluidine and 2,6-xylidine, respectively, using HPLC. Each data point represents the mean ± S.D. of triplicate determinations.

protein, respectively, whereas CES2 did not display any lidocaine hydrolase activity (Table 1). AADAC did not display hydrolase activities for either prilocaine or lidocaine. These results indicate that the metabolic efficiency of prilocaine hydrolysis by CES1A was higher than that of lidocaine hydrolysis. CES2 participated in prilocaine hydrolysis but not lidocaine hydrolysis.

Formation of Met-Hb by Prilocaine or Lidocaine and Their Metabolites. To investigate Met-Hb formation in vitro, prilocaine, lidocaine, or their hydrolyzed metabolites, *o*-toluidine and 2,6-xylidine, were incubated with HLM, an NADPH-GS, and mouse red blood cells for 0–120 minutes. Met-Hb formation was linear with respect to incubation time (1 mM prilocaine or lidocaine <120 minutes, 1 mM *o*-toluidine or 2,6-xylidine <60 minutes) (Fig. 2A).

To compare the induction potency of Met-Hb formation among prilocaine, lidocaine, *o*-toluidine, and 2,6-xylidine, the compounds were incubated at various concentrations (Fig. 2B). Met-Hb formation increased in a concentration-dependent manner. *o*-Toluidine and 2,6-xylidine more efficiently induced Met-Hb formation, compared

TABLE 1

Kinetic parameters of the hydrolase activities of prilocaine and lidocaine

Data are the mean ± S.D. of triplicate determinations.

Drug	Enzyme Source	K_m	V_{max}	CL_{int}
		mM	*nmol/min/mg protein*	*μl/min/mg protein*
Prilocaine	HLM	1.15 ± 0.01	2.46 ± 0.04	2.14 ± 0.04
	CES1A	0.31 ± 0.01	0.40 ± 0.01	1.29 ± 0.04
	CES2	0.39 ± 0.01	0.10 ± 0.00	0.26 ± 0.00
	AADAC	ND	ND	—
Lidocaine	HLM	0.96 ± 0.06	0.62 ± 0.01	0.66 ± 0.03
	CES1A	0.35 ± 0.06	0.14 ± 0.00	0.40 ± 0.02
	CES2	ND	ND	—
	AADAC	ND	ND	—

ND, not detected.

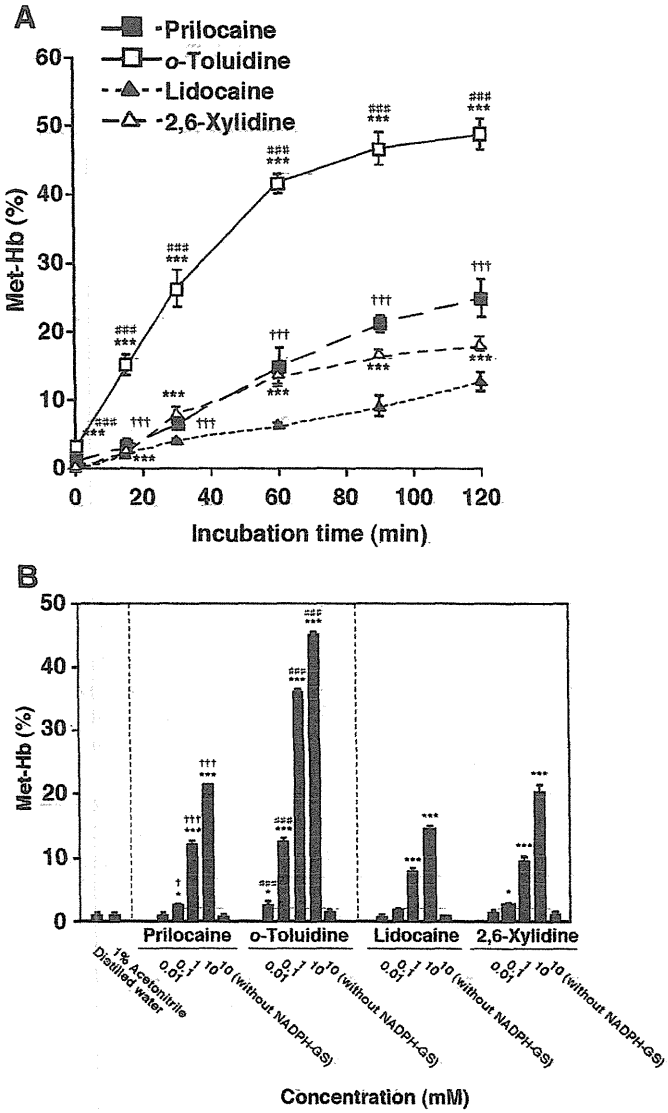

Fig. 2. (A) Time-dependent prilocaine-, lidocaine-, *o*-toluidine–, and 2,6-xylidine–induced Met-Hb formation. Prilocaine, lidocaine, and their hydrolyzed metabolites (1 mM) were incubated for 0–120 minutes with HLM (1.0 mg/ml), an NADPH-GS, and mouse red blood cells. Each data point represents the mean ± S.D. of triplicate determinations. Differences in Met-Hb formation, compared with the corresponding parent compounds at the same incubation time, were considered to be significant at $^{***}P < 0.001$. Differences in prilocaine- and lidocaine-induced Met-Hb formation at the same incubation time were considered to be significant at $^{\dagger\dagger\dagger}P < 0.001$. Differences in *o*-toluidine– and 2,6-xylidine–induced Met-Hb formation at the same incubation time were considered to be significant at $^{\#\#\#}P < 0.001$. (B) Concentration-dependent prilocaine-, lidocaine-, *o*-toluidine–, and 2,6-xylidine–induced Met-Hb formation. Prilocaine, lidocaine, and their hydrolyzed metabolites (0.01–10 mM) were incubated with HLM (1.0 mg/ml), an NADPH-GS, and mouse red blood cells for 60 minutes. Each column represents the mean ± S.D. of triplicate determinations. Differences in Met-Hb formation, compared with the corresponding vehicle-treated controls, were considered to be significant at $^{*}P < 0.05$; $^{***}P < 0.001$. Differences in prilocaine- and lidocaine-induced Met-Hb formation at the same concentration were considered to be significant at $^{\dagger}P < 0.05$; $^{\dagger\dagger\dagger}P < 0.001$. Differences in *o*-toluidine– and 2,6-xylidine–induced Met-Hb formation at the same concentration were considered to be significant at $^{\#\#\#}P < 0.001$.

with their corresponding parent drugs. This result suggested that the hydrolyzed metabolites enhanced prilocaine- or lidocaine-induced Met-Hb formation. Prilocaine-induced Met-Hb formation was significantly higher than lidocaine-induced formation at each concentration that was greater than 0.1 mM. In the same manner, *o*-toluidine–induced Met-Hb formation was significantly higher than 2,6-xylidine–induced

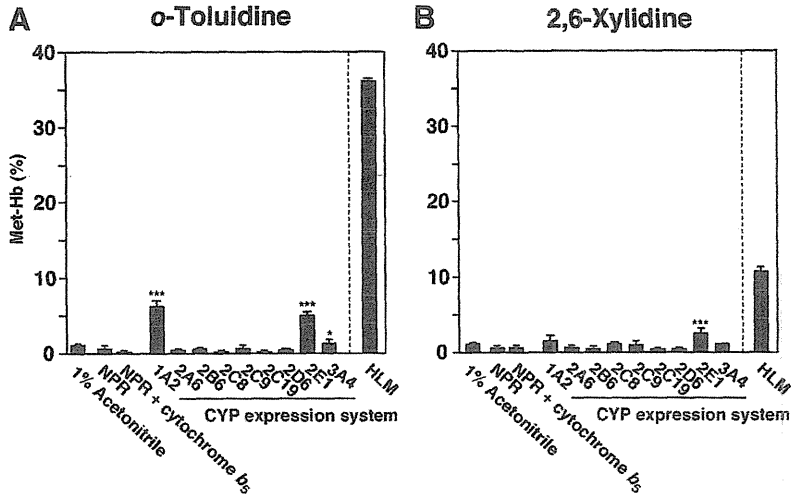

Fig. 3. The effects of P450 (CYP) enzymes on *o*-toluidine– and 2,6-xylidine–induced Met-Hb formation. Each individual recombinant human P450 expression system (25 pmol P450/ml) or HLM (1.0 mg/ml) was incubated with 1 mM *o*-toluidine (A) or 2,6-xylidine (B), an NADPH-GS, and mouse red blood cells for 60 minutes. Each column represents the mean ± S.D. of triplicate determinations. Differences in Met-Hb formation, compared with NPR or NPR + cytochrome b_5 (control supersomes expressing no P450s), were considered to be significant at $^*P < 0.05$; $^{***}P < 0.001$.

formation at each concentration that was greater than 0.1 mM. The increased Met-Hb formation that was induced by prilocaine, lidocaine, and their hydrolyzed metabolites was not observed in the absence of an NADPH-GS (Fig. 2B). These results suggest that the potency of prilocaine to induce Met-Hb formation was approximately 1.5-fold higher than that of lidocaine at the same concentration and that the NADPH-dependent enzymes that are expressed in HLM are essential for Met-Hb formation.

Met-Hb Formation after the Metabolic Activation of *o*-Toluidine and 2,6-Xylidine by Human P450(s). As outlined above, NADPH-dependent enzyme(s) are essential for prilocaine- and lidocaine-induced Met-Hb formation. Therefore, the involvement of representative NADPH-dependent enzymes (the P450 enzymes) in *o*-toluidine and 2,6-xylidine metabolism was investigated (Fig. 3). Either *o*-toluidine or 2,6-xylidine (1 mM) was incubated with recombinant human P450s, an NADPH-GS, and mouse red blood cells. *o*-Toluidine–induced Met-Hb formation was significantly increased by CYP1A2 (6.2% ± 0.7%), CYP2E1 (5.0% ± 0.4%), and CYP3A4 (1.3% ± 0.5%), and 2,6-xylidine–induced Met-Hb formation was increased by CYP2E1 (2.3% ± 0.8%).

Prilocaine- and Lidocaine-Induced Met-Hb Formation Inhibition Analyses in the Presence of Esterase Inhibitors. To investigate the involvement of human CES in prilocaine- and lidocaine-induced methemoglobinemia, inhibition analyses were performed with DFP and BNPP, which are potent CES inhibitors (Watanabe et al., 2009) (Fig. 4). The hydrolase activities of prilocaine and lidocaine (1 mM) in HLM (1.0 mg/ml) were preliminarily confirmed by HPLC to be completely inhibited by 10 μM DFP and 10 μM BNPP (unpublished data). When prilocaine and lidocaine (10 mM) were incubated with HLM, an NADPH-GS, and mouse red blood cells in the presence of DFP or BNPP (100 μM), both prilocaine- and lidocaine-induced Met-Hb formation were decreased (prilocaine, percentage of control: 31.6% in the presence of DFP and 34.0% in the presence of BNPP; lidocaine, percentage of control: 56.6% in the presence of DFP and 56.6% in the presence of BNPP) (Fig. 4). DFP and BNPP did not alter Met-Hb formation (unpublished data). Thus, CES were determined to be involved in Met-Hb formation.

Met-Hb Formation after the Metabolic Activation of Prilocaine and Lidocaine by Human P450(s). As shown in Fig. 4, DFP and BNPP could not completely inhibit prilocaine- and lidocaine-induced Met-Hb formation, suggesting that the metabolic activation of prilocaine and lidocaine by P450 enzyme(s) may mediate Met-Hb formation in the absence of hydrolysis. When prilocaine and lidocaine (10 mM) were incubated with representative recombinant human P450s, an NADPH-GS, and mouse red blood cells, Met-Hb formation increased in the presence of CYP3A4 (1.7% ± 0.2% for prilocaine and 1.1% ± 0.4% for lidocaine) (Fig. 5). These results suggest that prilocaine- and lidocaine-induced Met-Hb formation in the absence of hydrolysis is catalyzed by metabolic activation by human CYP3A4.

Normalizing Met-Hb Formation by P450 Levels in HLM. Because each P450 enzyme is expressed at different levels in HLM, we were unable to simply compare the contribution of each P450 enzyme to prilocaine-, lidocaine-, *o*-toluidine–, or 2,6-xylidine–induced Met-Hb formation in HLM with use of human P450 expression systems. Therefore, to estimate the contributions of P450 enzymes in HLM, Met-Hb formation in the presence of recombinant P450 expression systems was normalized by the levels of each P450 enzyme in HLM (Fig. 6). For *o*-toluidine– and 2,6-xylidine–induced Met-Hb formation, CYP2E1 had the highest contribution in HLM,

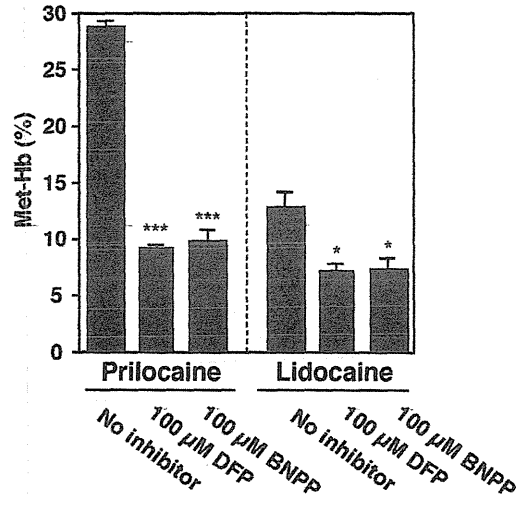

Fig. 4. The effects of DFP or BNPP on prilocaine- and lidocaine-induced Met-Hb formations. HLM (1.0 mg/ml) were incubated with prilocaine or lidocaine (10 mM), an NADPH-GS, and mouse red blood cells for 120 minutes. The concentration of DFP or BNPP was 100 μM. Each column represents the mean ± S.D. of triplicate determinations. Prilocaine- and lidocaine-induced Met-Hb formation in the absence of inhibitors was 28.8% ± 0.5% and 12.9% ± 1.3%, respectively. Differences compared with the controls lacking inhibitor were considered to be significant at $^*P < 0.05$; $^{***}P < 0.001$.

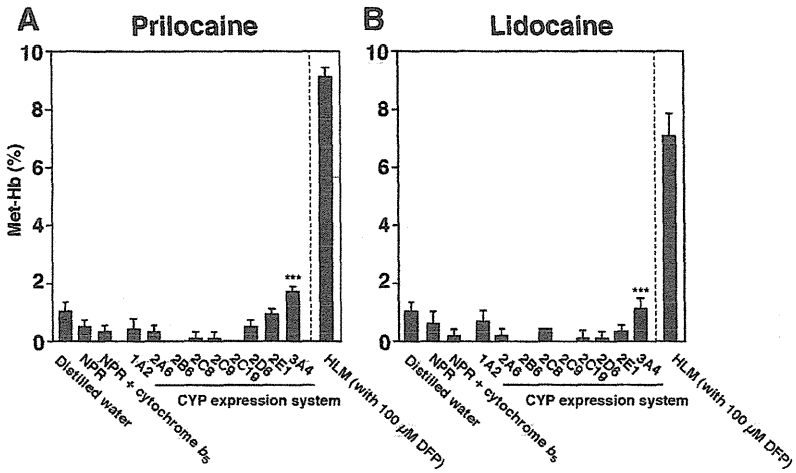

Fig. 5. The effects of P450 (CYP) enzymes on prilocaine- and lidocaine-induced Met-Hb formation without hydrolysis pathway. Each individual recombinant human P450 expression system (25 pmol P450/ml) or HLM (1.0 mg/ml) was incubated with 10 mM prilocaine (A) or lidocaine (B), an NADPH-GS, and mouse red blood cells for 120 minutes. Each column represents the mean ± S.D. of triplicate determinations. Differences in Met-Hb formation, compared with NPR or NPR + cytochrome b_5 (control supersomes expressing no P450s), were considered to be significant at $^*P < 0.05$; $^{***}P < 0.001$.

whereas CYP1A2 and CYP3A4 had relatively low contributions (Fig. 6, A and B). For prilocaine- and lidocaine-induced Met-Hb formation, CYP3A4 had the highest contribution in HLM (Fig. 6, C and D). Although flavin-containing monooxygenase is also known to be an NADPH-dependent enzyme, Met-Hb formation that was induced by prilocaine, lidocaine, and their hydrolyzed metabolites in HLM was not inhibited by 1 mM methimazole, which is a competitive flavin-containing monooxygenase inhibitor (unpublished data) (Rawden et al., 2000). Thus, CYP2E1 was determined to contribute highly to *o*-toluidine– and 2,6-xylidine–induced Met-Hb formation, whereas CYP3A4 was determined to contribute highly to prilocaine- and lidocaine-induced Met-Hb formation.

Met-Hb Formation Inhibition Analyses after the Incubation of Prilocaine, Lidocaine, and Their Hydrolyzed Metabolites with Anti-P450 Antibodies. To further investigate the contributions of CYP1A2, CYP2E1, and CYP3A4 to the *o*-toluidine– and 2,6-xylidine–induced Met-Hb formation in HLM, inhibition analyses were performed using anti-P450 antibodies (Fig. 7A). *o*-Toluidine– and 2,6-xylidine–induced Met-Hb formation were markedly decreased by incubation with an anti-CYP2E1 antibody (from 19.5% ± 0.6% to 7.1% ± 0.4% for

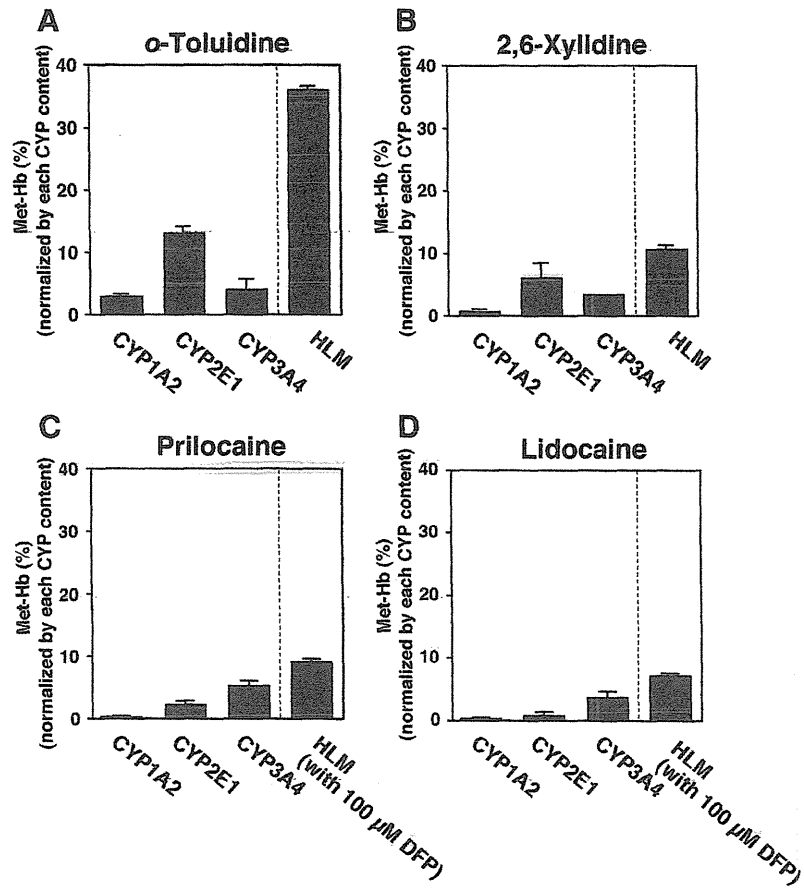

Fig. 6. Met-Hb formation normalized by the levels of each P450 (CYP) in HLM. Met-Hb formation was normalized by the levels of each P450 and calculated according to the equation described in *Materials and Methods*. Prilocaine, lidocaine (10 mM) (A and C), and their hydrolyzed metabolites (1 mM) (B and D) were incubated with each P450 expression system (25 pmol P450/ml), an NADPH-GS, and mouse red blood cells. The incubation time was 120 minutes (prilocaine and lidocaine) or 60 minutes (*o*-toluidine and 2,6-xylidine). Each column represents the mean ± S.D. of triplicate determinations.

o-toluidine and from 6.2% ± 0.3% to 2.6% ± 0.2% for 2,6-xylidine) and slightly decreased by incubation with an anti-CYP3A4 antibody (to 16.9% ± 0.5% for *o*-toluidine and to 4.3% ± 0.3% for 2,6-xylidine). Incubation with an anti-CYP1A2 antibody also slightly decreased 2,6-xylidine–induced Met-Hb formation (to 5.0% ± 0.5%).

To investigate the contribution of CYP3A4 to prilocaine- and lidocaine-induced Met-Hb formation in the absence of hydrolysis, inhibition analyses were performed using anti-P450 antibodies (Fig. 7B). When 100 μM DFP was used to inhibit CES enzyme activity, incubation with an anti-CYP3A4 antibody substantially decreased prilocaine- and lidocaine-induced Met-Hb formation (from 5.7% ± 0.4% to 0.6% ± 0.3% for prilocaine and from 3.4% ± 0.4% to 0.7% ± 0.2% for lidocaine).

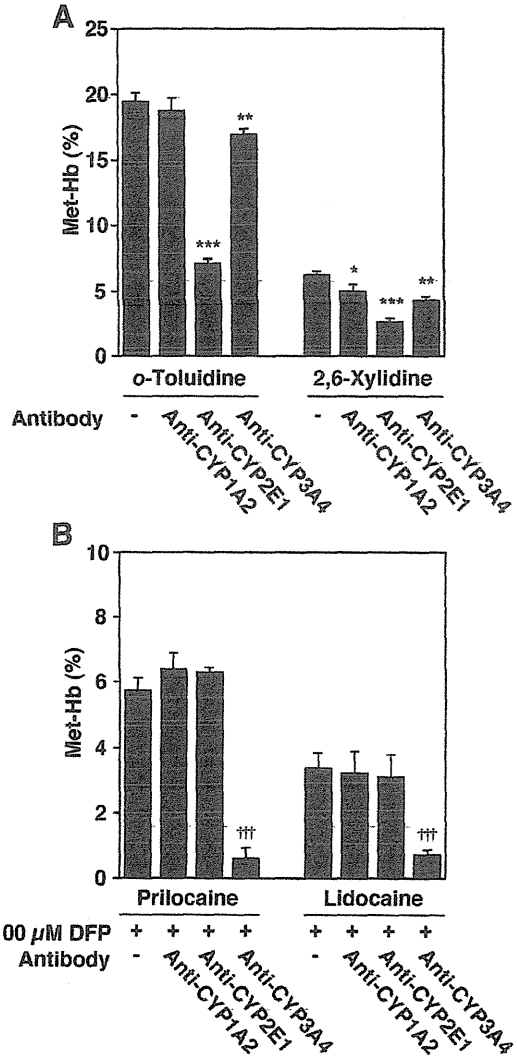

Fig. 7. Inhibitory effects of anti-human CYP1A2, CYP2E1, and CYP3A4 antibodies on *o*-toluidine–, 2,6-xylidine–, prilocaine-, and lidocaine-induced Met-Hb formations in HLM. HLM (0.5 mg/ml) were incubated with 1 mM *o*-toluidine, 1 mM 2,6-xylidine (A), 10 mM prilocaine, or 10 mM lidocaine (in the presence of 100 μM DFP) (B), an NADPH-GS, mouse red blood cells, and each P450 antibody. Met-Hb formation in the absence of antibody was 19.5% ± 0.6% (*o*-toluidine) and 6.2% ± 0.3% (2,6-xylidine), and Met-Hb formation in the absence of antibody but in the presence of DFP was 5.7% ± 0.4% (prilocaine) and 3.4% ± 0.4% (lidocaine). The incubation time was 120 minutes (prilocaine and lidocaine) and 60 minutes (*o*-toluidine and 2,6-xylidine). Each column represents the mean ± S.D. of triplicate determinations. Differences compared to control with no antibody were considered significant at $^{*}P < 0.05$; $^{**}P < 0.005$; and $^{***}P$ or $\dagger\dagger\dagger P < 0.001$.

Met-Hb Formation in the Presence of the Hydroxylated Metabolites of *o*-Toluidine and 2,6-Xylidine. 4-Hydroxy-*o*-toluidine, 6-hydroxy-*o*-toluidine, or 4-hydroxy-2,6-xylidine has been detected in human urine after the administration of prilocaine or lidocaine (Hjelm et al., 1972; Keenaghan and Boyes, 1972). To investigate whether these metabolites could induce Met-Hb formation, in vitro analyses were performed. 4-Hydroxy-*o*-toluidine–,6-hydroxy-*o*-toluidine–, and 4-hydroxy-2,6-xylidine–induced Met-Hb formation were markedly increased, in both the presence and the absence of an NADPH-GS (Fig. 8). A higher degree of Met-Hb formation was detected in the presence of these metabolites than in the presence of *o*-toluidine and 2,6-xylidine. Thus, it was suggested that these hydroxylated metabolites of *o*-toluidine and 2,6-xylidine were one of the causative factors underlying prilocaine- and lidocaine-induced methemoglobinemia.

Formation of the Hydroxylated Metabolites of *o*-Toluidine and 2,6-Xylidine in HLM. Because the hydroxylated metabolites of *o*-toluidine and 2,6-xylidine could induce Met-Hb formation, we investigated whether HLM could catalyze the hydroxylation of *o*-toluidine and 2,6-xylidine (Fig. 9, A and B). Data for these hydroxylase activities in HLM followed Michaelis-Menten kinetics. The K_m and V_{max} values for 4-hydroxylation of *o*-toluidine in HLM were 50.2 ± 2.8 μM and 0.61 ± 0.03 nmol/min/mg protein, respectively, resulting in a CL_{int} value of 12.2 ± 0.2 μl/min/mg protein. The K_m and V_{max} values for 6-hydrolxylation of *o*-toluidine in HLM were 70.3 ± 6.2 μM and 0.05 ± 0.00 nmol/min/mg protein, respectively, resulting in a CL_{int} value of 0.7 ± 0.1 μl/min/mg protein (Table 2). Thus, the CL_{int} value for 4-hydroxylation of *o*-toluidine in HLM was

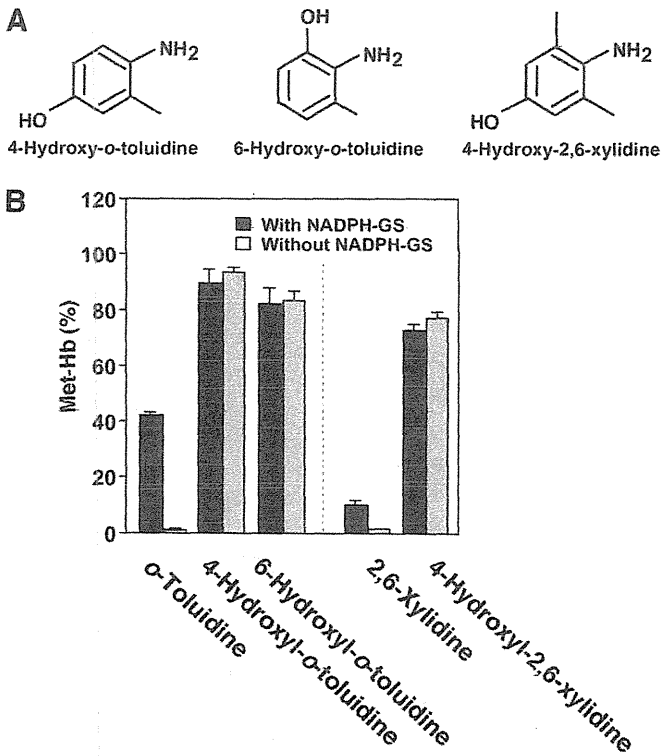

Fig. 8. (A) Chemical structures of 4-hydroxy-*o*-toluidine, 6-hydroxy-*o*-toluidine, and 6-hydroxy-2,6-xylidine. (B) Met-Hb formation induced by the hydroxylated metabolites of *o*-toluidine and 2,6-xylidine. *o*-Toluidine, 4-hydroxy-*o*-toluidine, 6-hydroxy-*o*-toluidine, 2,6-xylidine, or 4-hydroxy-2,6-xylidine (1 mM) was incubated with HLM (1.0 mg/ml) and mouse red blood cells in the presence or absence of an NADPH-GS for 60 minutes. Each column represents the mean ± S.D. of triplicate determinations.

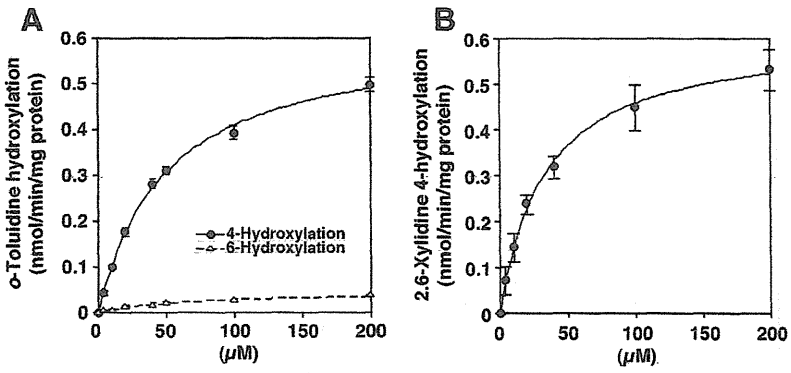

Fig. 9. Kinetic analyses of *o*-toluidine and 2,6-xylidine hydroxylase activities in HLM. HLM (0.4 mg/ml) was incubated with *o*-toluidine (A) and 2,6-xylidine (B) for 30 minutes. *o*-Toluidine and 2,6-xylidine hydroxylase activities were measured by quantitative analyses of 4- or 6-hydroxyl-*o*-toluidine and 4-hydroxy-2,6-xylidine, respectively, using HPLC. Each data point represents the mean ± S.D. of triplicate determinations.

shown to be 18-fold higher than that for 6-hydroxylation. The K_m and V_{max} values for 4-hydroxylation of 2,6-xylidine in HLM were 34.1 ± 5.1 μM and 0.61 ± 0.04 nmol/min/mg protein, respectively, resulting in a CL_{int} value of 18.3 ± 3.4 μl/min/mg protein. These results indicate that *o*-toluidine and 2,6-xylidine were efficiently metabolized to their hydroxylated forms in HLM.

Inhibition Analyses of *o*-Toluidine and 2,6-Xylidine Hydroxylase Activities in the Presence of Anti-P450 Antibodies. To further investigate the contributions of CYP1A2, CYP2E1, and CYP3A4 to *o*-toluidine and 2,6-xylidine hydroxylation in HLM, inhibition analyses were performed using anti-P450 antibodies (Fig. 10). *o*-Toluidine 4- and 6-hydroxylase activities were markedly decreased (percentage of control: 35.4% ± 1.6% for *o*-toluidine 4-hydroxylation and 47.1% ± 2.3% for *o*-toluidine 6-hydroxylation) by incubation with an anti-CYP2E1 antibody. 2,6-Xylidine 4-hydroxylase activity was also markedly decreased by incubation with an anti-CYP2E1 (percentage of control: 25.6% ± 0.9%) and slightly decreased by incubation with an anti-CYP3A4 antibody (percentage of control: 92.9% ± 0.3%). Thus, it was suggested that CYP2E1 could mainly catalyze *o*-toluidine and 2,6-xylidine hydroxylations, leading to Met-Hb formation.

Prilocaine- and Lidocaine-Induced Met-Hb Formation in Human Red Blood Cells. In the aforementioned Met-Hb formation analyses, mouse red blood cells were used. To assess species-specific differences in Met-Hb formation between mice and humans, an analysis using human red blood cells that were obtained from 5 individuals was conducted as follows: prilocaine or lidocaine (10 mM) was incubated with HLM, an NADPH-GS, and individual human red blood cells that had been obtained from the five healthy donors. The levels of Met-Hb formation in the absence of prilocaine or lidocaine were 0.6–1.5% (mean, 1.1%). High Met-Hb formation was observed after incubation with both prilocaine and lidocaine [prilocaine: mean, 34.8% (26.8–41.5%); lidocaine: mean, 9.9% (9.0–11.3%)], but the formation of Met-Hb was significantly decreased by incubation with 100 μM DFP [prilocaine: mean, 7.6% (6.8–8.6%); lidocaine: mean, 6.4% (5.1–7.4%)] (Fig. 11). This result was similar to that obtained using mouse red blood cells (Fig. 4). These results indicate the comparable Met-Hb formation sensitivity between human and mouse red blood cells.

TABLE 2

Kinetic parameters of the hydroxylase activities of *o*-toluidine and 2,6-xylidine

HLM: 0.4 mg/ml. Data are the mean ± S.D. of triplicate determinations.

Hydroxylase Reaction	K_m	V_{max}	CL_{int}
	μM	*nmol/min/mg protein*	*μl/min/mg protein*
o-Toluidine			
4-Hydroxylation	50.2 ± 2.8	0.61 ± 0.03	12.2 ± 0.2
6-Hydroxylation	70.3 ± 6.2	0.05 ± 0.00	0.7 ± 0.1
2,6-Xylidine			
4-Hydroxylation	34.1 ± 5.1	0.61 ± 0.04	18.3 ± 3.4

Discussion

Prilocaine and lidocaine are typical amide-type local anesthetics that carry the risk of a serious adverse reaction known as methemoglobinemia (Maimo and Redick, 2004). Prilocaine and lidocaine are hydrolytically metabolized to the aromatic amines *o*-toluidine and 2,6-xylidine, respectively. Although these metabolites were suspected to be causes of prilocaine- and lidocaine-induced methemoglobinemia (Neuhaeuser et al., 2008), the enzymes responsible for Met-Hb formation remained to be characterized. In the present study, we found that metabolic activation by human CES, CYP2E1, and CYP3A4 was involved in prilocaine- and lidocaine-induced methemoglobinemia.

We demonstrated that prilocaine was hydrolyzed by CES1A and CES2, whereas lidocaine was specifically hydrolyzed by CES1A (Fig. 1), and that hydrolysis reactions that were catalyzed by CES enzymes enhanced prilocaine- and lidocaine-induced Met-Hb formation (Figs. 2 and 4). Because prilocaine and lidocaine hydrolase activities were detected in HLM, but not in human plasma where cholinesterases and paraoxonases are expressed (unpublished data), these enzymes could be excluded from the candidate enzymes catalyzing their hydrolysis. Recombinant human AADAC showed no activity (Fig. 1; Table 1). Moreover, prilocaine and lidocaine hydrolase activities at 1 mM were completely inhibited by 100 μM DFP and BNPP (unpublished data), which are potent CES inhibitors (Watanabe et al., 2009). Collectively, these results suggest that CES enzymes are major enzymes that are responsible for the hydrolysis of prilocaine and lidocaine.

Met-Hb formation after the incubation of the parent compounds (prilocaine and lidocaine) with HLM was lower than that after incubation of their hydrolyzed metabolites (*o*-toluidine and 2,6-xylidine) (Fig. 2). Prilocaine- and lidocaine-induced Met-Hb formation was significantly decreased by DFP and BNPP (Fig. 4), indicating that CES enzymes may be involved in the prilocaine- and lidocaine-induced Met-Hb formation. When metabolic efficiency was analyzed, prilocaine was shown to be more efficiently hydrolyzed in HLM than was lidocaine (Fig. 1, A and B). Furthermore, prilocaine- and *o*-toluidine–induced Met-Hb formation was higher than that induced by incubating lidocaine and 2,6-xylidine (Fig. 2, A and B). These results support the previous report (Guay, 2009), which indicates that the number of prilocaine-related methemoglobinemia episodes is higher than that of lidocaine-related methemoglobinemia.

We considered the possibility that hydrolysis may not be the sole cause of prilocaine- and lidocaine-induced methemoglobinemia, because Met-Hb formation was not completely inhibited by DFP and BNPP.

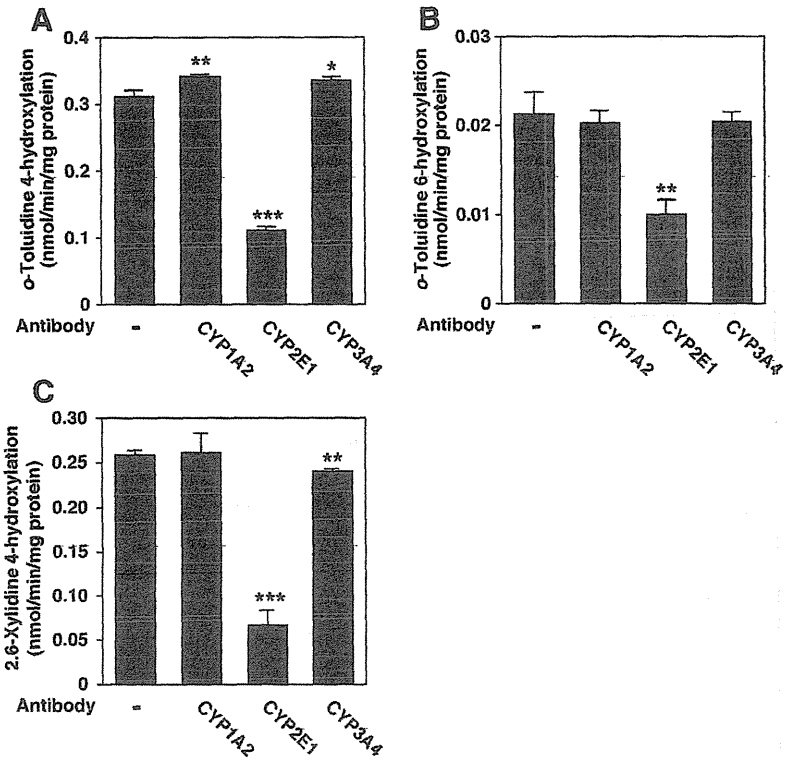

Fig. 10. Inhibitory effects of anti-human CYP1A2, CYP2E1, and CYP3A4 antibodies on *o*-toluidine- or 2,6-xylidine hydroxylation in HLM. HLM (0.4 mg/ml) was incubated with 50 μM *o*-toluidine or 30 μM 2,6-xylidine, an NADPH-GS, and each P450 antibody for 30 minutes. The control activities for *o*-toluidine-4-hydroxylation (A), *o*-toluidine-6-hydroxylation (B), and 2,6-xylidine-4-hydroxylation (C) were 0.31 ± 0.01, 0.02 ± 0.00, and 0.26 ± 0.00 nmol/min/mg protein, respectively. Each column represents the mean ± S.D. of triplicate determinations. Differences compared to control with no antibody were considered significant at $^{*}P < 0.05$; $^{**}P < 0.005$; and $^{***}P < 0.001$.

Supporting this assumption, we observed that metabolism by P450 enzymes was also required for prilocaine- and lidocaine-induced Met-Hb formation in the presence and absence of the hydrolysis reaction (Figs. 2, 3, and 5–7). Human P450 enzymes, which are major NADPH-dependent enzymes, account for ~75% of the metabolism of clinical drugs (Guengerich, 2008). In the absence of an NADPH-GS, Met-Hb formation after incubation with prilocaine, lidocaine, and their hydrolyzed metabolites was not increased (Fig. 2B). In fact, we demonstrated that Met-Hb formation was increased by CYP3A4 (prilocaine and lidocaine) by using recombinant P450 enzymes in the absence of the hydrolysis reaction (Fig. 5). The formation of Met-Hb after incubation with the hydrolyzed metabolites was indeed increased by CYP1A2, CYP2E1, and CYP3A4 (*o*-toluidine) or CYP2E1 (2,6-xylidine) (Fig. 3). When we accounted for the levels of each P450 enzyme in HLM, CYP2E1 appeared to contribute highly to the formations of Met-Hb after incubation with the hydrolyzed metabolites (Fig. 6). These data were consistent with those obtained in the analyses that were conducted in the presence of anti-P450 antibodies (Fig. 7A). Met-Hb formation in the presence of HLM was similar to the sum of Met-Hb formation by each of the individual P450 expression systems (Fig. 6), indicating that these P450 enzymes may be responsible for Met-Hb formation in the presence of prilocaine, lidocaine, *o*-toluidine, or 2,6-xylidine in the presence and absence of the hydrolysis reaction. Collectively, our data indicate that two metabolic pathways, the hydrolysis pathway, which is catalyzed by CES enzymes and CYP2E1, and the nonhydrolysis pathway, which is catalyzed by CYP3A4, may be involved in prilocaine- and lidocaine-induced methemoglobinemia (Fig. 12).

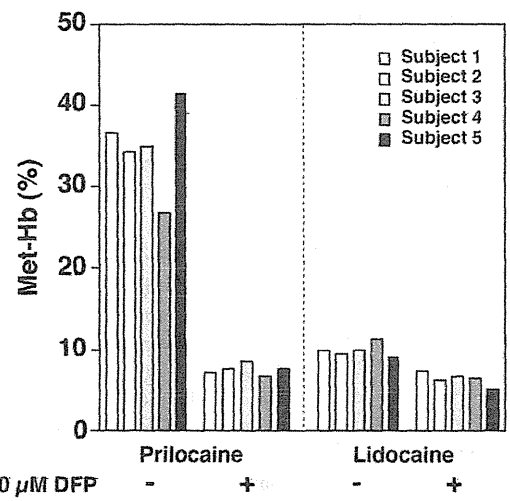

Fig. 11. Prilocaine- and lidocaine-induced Met-Hb formation after incubation with human red blood cells in the absence or presence of 100 μM DFP. HLM (1.0 mg/ml) was incubated for 120 minutes with prilocaine or lidocaine (10 mM), an NADPH-GS, and human red blood cells that had been obtained from five healthy individuals.

By comparing the decreased levels of Met-Hb after incubation with DFP to the residual formation of Met-Hb (Fig. 4), the contributions of the hydrolytic and nonhydrolytic metabolic pathways to prilocaine- and lidocaine-induced Met-Hb formation in HLM can be roughly predicted. The decreases in prilocaine- and lidocaine-induced Met-Hb formation were 2.16- and 0.82-fold greater, respectively, than the residual formation of Met-Hb. Thus, the hydrolysis of prilocaine by CES enzymes highly contributed to prilocaine-induced formation, whereas the hydrolytic and nonhydrolytic pathways of lidocaine seemed to contribute equally to Met-Hb formation.

Methemoglobinemia is reported to be induced by certain types of clinically used drugs, including the analgesic antipyretic phenacetin, the antileprosy drug dapsone, and the antibiotic sulfamethoxazole (Reilly et al., 1999; Ganesan et al., 2010; Kobayashi et al., 2012), which all possess an aromatic amine moiety. *N*-Hydroxylamines, which are *N*-hydroxylated metabolites of aromatic amines, were suspected to be a cause of aromatic amine-induced methemoglobinemia (Spooren and

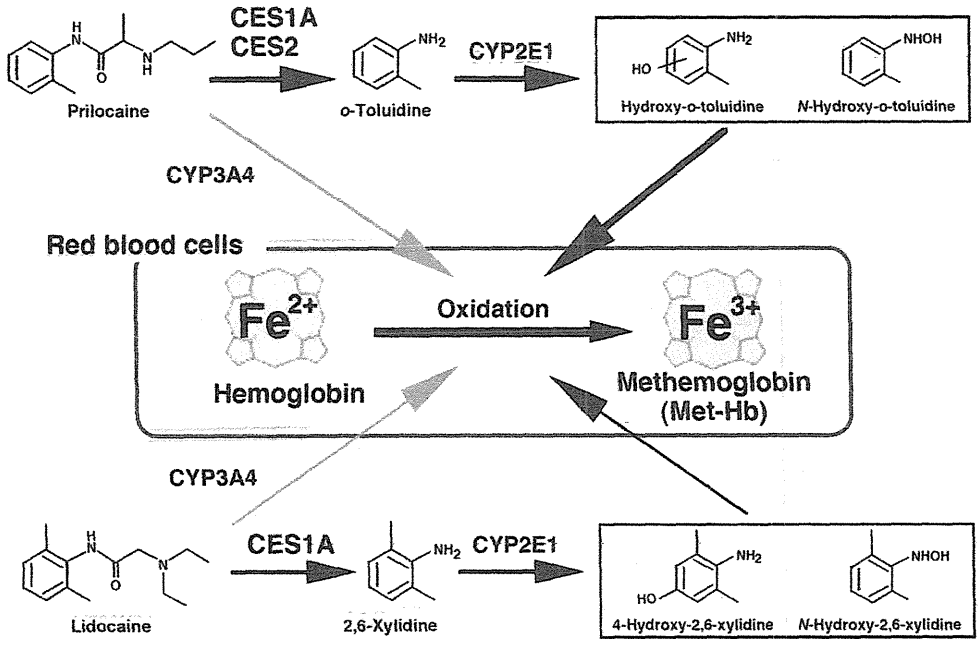

Fig. 12. Mechanisms suggested to underlie prilocaine- and lidocaine-induced Met-Hb formation. Two metabolic pathways are proposed: the hydrolysis pathway, which is mediated by CES and CYP2E1, and the nonhydrolysis pathway, which is mediated by CYP3A4.

Evelo, 2000). For instance, in vitro experimental data indicate that dapsone-hydroxylamine, which is an *N*-hydroxylated metabolite of dapsone that is catalyzed by CYP2C19, CYP2E1, and CYP3A4, may cause dapsone-induced methemoglobinemia (Reilly et al., 1999). Therefore, *N*-hydroxyl-*o*-toluidine and *N*-hydroxyl-2,6-xylidine, which are *N*-hydroxylated metabolites of *o*-toluidine and 2,6-xylidine, respectively, may cause Met-Hb formation after exposure to *o*-toluidine and 2,6-xylidine. Because *N*-hydroxylamines are generally unstable (Fuller, 1978), *N*-hydroxyl-*o*-toluidine and *N*-hydroxyl-2,6-xylidine could not be obtained. 4-Hydroxy-*o*-toluidine and 6-hydroxy-*o*-toluidine or 4-hydroxy-2,6-xylidine (Fig. 8A) have been detected in human urine after the administration of prilocaine or lidocaine, respectively (Hjelm et al., 1972; Keenaghan and Boyes, 1972). We also confirmed that *o*-toluidine and 2,6-xylidine were converted to the hydroxylated metabolites 4- and 6-hydroxy-*o*-toluidine or 4-hydroxy-2,6-xylidine in HLM (Fig. 9) and that hydroxylation of *o*-toluidin and 2,6-xylidine was mainly catalyzed by CYP2E1 (Fig. 10). These hydroxylated metabolites could efficiently induce Met-Hb formation in the absence of an NADPH-GS (Fig. 8B), suggesting that 4- and 6-hydroxy-*o*-toluidine or 4-hydroxy-2,6-xylidine may also cause Met-Hb formation after exposure to *o*-toluidine and 2,6-xylidine, respectively. Although *o*-toluidine more efficiently induced Met-Hb formation than did 2,6-xylidine (Fig. 2), the metabolic efficiency of *o*-toluidine 4-hydroxylation was shown to be lower than that of 2,6-xylidine 4-hydroxylation (Table 2). This discrepancy may be accounted for by the *N*-hydroxylated metabolites. Because we could not compare the induction potencies of Met-Hb formation between the *N*-hydroxylated metabolites and the other hydroxylated metabolites, the metabolite that contributed to Met-Hb formation to the greatest degree could not be determined.

As shown in Figs. 6, C and D, and 7B, CYP3A4 may be involved in prilocaine- and lidocaine-induced Met-Hb formation in the absence of the hydrolysis pathway. Lidocaine is known to be metabolized to monoethylglycinexylidide by CYP3A4, but we confirmed that little Met-Hb was formed after incubation with monoethylglycinexylidide (Supplemental Fig. 1). In addition, lidocaine is metabolized to 3-hydroxylidocaine, but this metabolite was excluded as a potential cause of Met-Hb formation, because it is formed by CYP1A2 and CYP3A4 (Wang et al., 2000). P450 enzymes have not been previously reported to participate in the metabolism of prilocaine. It will be worthwhile to identify the metabolites of prilocaine and lidocaine that cause methemoglobinemia and are catalyzed by CYP3A4 in the near future.

An in vitro assay to determine Met-Hb formation used human red blood cells that had been obtained from five individuals, resulting in comparable sensitivity for Met-Hb formation between human and mouse red blood cells (Figs. 4 and 11). Vasters et al. (2006) reported that interindividual differences in the Met-Hb levels (17.1-fold) varied by more than the variation observed after different dosages of prilocaine (1.4-fold). Neuhaeuser et al. (2008) reported that there were large interindividual variations in Met-Hb levels (8.8-fold) despite the similar dosages of lidocaine that had been administered to patients. In this study, no interindividual variability in Met-Hb formation was observed in individual red blood cells that were treated with prilocaine and lidocaine (Fig. 11). Therefore, we suggest that interindividual variations in Met-Hb formation after treatment with prilocaine and lidocaine were not attributable to hemoglobin in red blood cells per se, but rather to the metabolic potencies of enzymes, CES, and P450s, and Met-Hb reductases.

In conclusion, the present study clarified that two metabolic pathways, the hydrolysis pathway, which means the hydroxylation by CYP2E1 after the hydrolysis by CES(s), and the nonhydrolysis pathway, which is catalyzed by CYP3A4, were involved in prilocaine- and lidocaine-induced methemoglobinemia. Furthermore, the catalytic efficiencies of prilocaine and lidocaine metabolism may be involved in the different incidences of methemoglobinemia that were observed for prilocaine and lidocaine. The results obtained in this study will provide valuable information regarding the importance of CES and P450 enzymes in drug toxicity.

Authorship Contributions

Participated in research design: Higuchi, Fukami, Nakajima, Yokoi.
Conducted experiment: Higuchi, Fukami.
Contributed new reagent or analytic tools: Higuchi, Fukami.
Performed data analysis: Higuchi.
Wrote or contributed to the writing of the manuscript: Higuchi, Fukami, Yokoi.

References

Chauret N, Gauthier A, and Nicoll-Griffith DA (1998) Effect of common organic solvents on in vitro cytochrome P450-mediated metabolic activities in human liver microsomes. Drug Metab Dispos 26:1-4.

Climie CR, McLean S, Starmer GA, and Thomas J (1967) Methaemoglobinaemia in mother and foetus following continuous epidural analgesia with prilocaine. Clinical and experimental data. *Br J Anaesth* **39**:155–160.

Fukami T, Katoh M, Yamazaki H, Yokoi T, and Nakajima M (2008) Human cytochrome P450 2A13 efficiently metabolizes chemicals in air pollutants: naphthalene, styrene, and toluene. *Chem Res Toxicol* **21**:720–725.

Fukami T, Nakajima M, Sakai H, Katoh M, and Yokoi T (2007) CYP2A13 metabolizes the substrates of human CYP1A2, phenacetin, and theophylline. *Drug Metab Dispos* **35**:335–339.

Fukami T, Takahashi S, Nakagawa N, Maruichi T, Nakajima M, and Yokoi T (2010) In vitro evaluation of inhibitory effects of antidiabetic and antihyperlipidemic drugs on human carboxylesterase activities. *Drug Metab Dispos* **38**:2173–2178.

Fukami T and Yokoi T (2012) The emerging role of human esterases. *Drug Metab Pharmacokinet* **27**:466–477.

Fuller RW (1978) Structure-activity relationships among the halogenated amphetamines. *Ann N Y Acad Sci* **305**:147–159.

Ganesan S, Sahu R, Walker LA, and Tekwani BL (2010) Cytochrome P450-dependent toxicity of dapsone in human erythrocytes. *J Appl Toxicol* **30**:271–275.

Guay J (2009) Methemoglobinemia related to local anesthetics: a summary of 242 episodes. *Anesth Analg* **108**:837–845.

Guengerich FP (2008) Cytochrome p450 and chemical toxicology. *Chem Res Toxicol* **21**:70–83.

Hjelm M, Ragnarsson B, and Wistrand P (1972) Biochemical effects of aromatic compounds. 3. Ferrihaemoglobinaemia and the presence of *p*-hydroxy-*o*-toluidine in human blood after the administration of prilocaine. *Biochem Pharmacol* **21**:2825–2834.

Imai T, Taketani M, Shii M, Hosokawa M, and Chiba K (2006) Substrate specificity of carboxylesterase isozymes and their contribution to hydrolase activity in human liver and small intestine. *Drug Metab Dispos* **34**:1734–1741.

Keenaghan JB and Boyes RN (1972) The tissue distribution, metabolism and excretion of lidocaine in rats, guinea pigs, dogs and man. *J Pharmacol Exp Ther* **180**:454–463.

Kobayashi Y, Fukami T, Higuchi R, Nakajima M, and Yokoi T (2012) Metabolic activation by human arylacetamide deacetylase, CYP2E1, and CYP1A2 causes phenacetin-induced methemoglobinemia. *Biochem Pharmacol* **84**:1196–1206.

Kreutz RW and Kinni ME (1983) Life-threatening toxic methemoglobinemia induced by prilocaine. *Oral Surg Oral Med Oral Pathol* **56**:480–482.

Lindstrom HV, Bowie WC, Wallace WC, Nelson AA, and Fitzhugh OG (1969) The toxicity and metabolism of mesidine and pseudocumidine in rats. *J Pharmacol Exp Ther* **167**:223–234.

Lipkind GM and Fozzard HA (2005) Molecular modeling of local anesthetic drug binding by voltage-gated sodium channels. *Mol Pharmacol* **68**:1611–1622.

Maimo G and Redick E (2004) Recognizing and treating methemoglobinemia: a rare but dangerous complication of topical anesthetic or nitrate overdose. *Dimens Crit Care Nurs* **23**:116–118.

Moore TJ, Walsh CS, and Cohen MR (2004) Reported adverse event cases of methemoglobinemia associated with benzocaine products. *Arch Intern Med* **164**:1192–1196.

Nakajima A, Fukami T, Kobayashi Y, Watanabe A, Nakajima M, and Yokoi T (2011) Human arylacetamide deacetylase is responsible for deacetylation of rifamycins: rifampicin, rifabutin, and rifapentine. *Biochem Pharmacol* **82**:1747–1756.

Nakajima M, Tane K, Nakamura S, Shimada N, Yamazaki H, and Yokoi T (2002) Evaluation of approach to predict the contribution of multiple cytochrome P450s in drug metabolism using relative activity factor: effects of the differences in expression levels of NADPH-cytochrome P450 reductase and cytochrome $b_{(5)}$ in the expression system and the differences in the marker activities. *J Pharm Sci* **91**:952–963.

Neuhaeuser C, Weigand N, Schaaf H, Mann V, Christophis P, Howaldt HP, and Heckmann M (2008) Postoperative methemoglobinemia following infiltrative lidocaine administration for combined anesthesia in pediatric craniofacial surgery. *Paediatr Anaesth* **18**:125–131.

Onji Y and Tyuma I (1965) Methemoglobin formation by a local anesthetic and some related compounds. *Acta Anaesthesiol Scand Suppl* **16**:151–159.

Rawden HC, Kokwaro GO, Ward SA, and Edwards G (2000) Relative contribution of cytochromes P-450 and flavin-containing monoxygenases to the metabolism of albendazole by human liver microsomes. *Br J Clin Pharmacol* **49**:313–322.

Rehman HU (2001) Methemoglobinemia. *West J Med* **175**:193–196.

Reilly TP, Woster PM, and Svensson CK (1999) Methemoglobin formation by hydroxylamine metabolites of sulfamethoxazole and dapsone: implications for differences in adverse drug reactions. *J Pharmacol Exp Ther* **288**:951–959.

Rodriguez LF, Smolik LM, and Zbehlik AJ (1994) Benzocaine-induced methemoglobinemia: report of a severe reaction and review of the literature. *Ann Pharmacother* **28**:643–649.

Spooren AA and Evelo CT (2000) A study on the interaction between hydroxylamine analogues and oxyhemoglobin in intact erythrocytes. *Blood Cells Mol Dis* **26**:373–386.

Vasters FG, Eberhart LH, Koch T, Kranke P, Wulf H, and Morin AM (2006) Risk factors for prilocaine-induced methaemoglobinaemia following peripheral regional anaesthesia. *Eur J Anaesthesiol* **23**:760–765.

Wang JS, Backman JT, Taavitsainen P, Neuvonen PJ, and Kivistö KT (2000) Involvement of CYP1A2 and CYP3A4 in lidocaine *N*-deethylation and 3-hydroxylation in humans. *Drug Metab Dispos* **28**:959–965.

Watanabe A, Fukami T, Nakajima M, Takamiya M, Aoki Y, and Yokoi T (2009) Human arylacetamide deacetylase is a principal enzyme in flutamide hydrolysis. *Drug Metab Dispos* **37**:1513–1520.

Watanabe A, Fukami T, Takahashi S, Kobayashi Y, Nakagawa N, Nakajima M, and Yokoi T (2010) Arylacetamide deacetylase is a determinant enzyme for the difference in hydrolase activities of phenacetin and acetaminophen. *Drug Metab Dispos* **38**:1532–1537.

Address correspondence to: Dr. Tatsuki Fukami, Drug Metabolism and Toxicology, Faculty of Pharmaceutical Sciences, Kanazawa University, Kakuma-machi, Kanazawa 920-1192, Japan. E-mail: tatsuki@p.kanazawa-u.ac.jp